Discrete numerical schemes for stochastic shallow water models under location uncertainty

Pierre-Marie Boulvard, Etienne Mémin, Jacques Sainte-Marie

Discrete numerical schemes for stochastic shallow water models under location uncertainty

Pierre-Marie Boulvard[1,2], Etienne Mémin[1], and Jacques Sainte Marie[2]

[1]Université de Rennes, Inria, IRMAR – UMR CNRS 6625, Rennes, France
[2]Inria, Sorbonne Université, Université Paris Cité, CNRS, Laboratoire Jacques-Louis Lions, LJLL, F-75005 Paris, France

April 16, 2026

Abstract

To address the complexity of numerically simulating turbulent flows at large scale, stochastic modelling approaches, particularly those incorporating transport noise, have gained a lot of attraction. Building on a Newtonian framework derived from stochastic transport, the Location Uncertainty (LU) model introduces stochastic contributions into fluid dynamics while keeping naturally energy conservation through a fluctuation-dissipation equilibrium. From a numerical point of view, recent studies have highlighted the benefits of simplifying high-order temporal schemes for stochastic simulations by omitting certain terms, resulting in discrete schemes that closely mirror deterministic models. This work focuses on developing efficient discrete schemes for a stochastic shallow water model, particularly emphasizing "second-order" methods. These methods involve iterated double advection of noise, ensuring an implicit implementation of noise-associated diffusion, thus achieving a balanced energy dissipation at the discrete level. The proposed schemes extend entropy-conserving methods, providing a robust framework for modeling under location uncertainty. These schemes have been numerically assessed for both idealized and realistic test cases over ensembles of realizations. In the realistic case, the stochastic simulations have been compared against observational data, while in the idealized case they have been evaluated against ground-truth fields obtained from a higher-resolution deterministic simulation..

1 Introduction

Shallow water models are widely used for the description of geophysical dynamics (Zeitlin, 2018). They find extensive application for real-world situations

such as tsunami modelling, storm surge prevention, the evolution of long surface waves, internal waves, large-scale oceanic currents, and granular flows (Mangeney et al., 2007). Different versions of the shallow-water equations, also known as the Saint-Venant equations after their initial author (de Saint-Venant, 1871), offer simple models for the evolution of depth-averaged velocity components coupled with hydrostatic balance assumption (Gerbeau and Perthame, 2001; Marche, 2007). This simple yet expressive model allows for the representation of discontinuities such as shocks. However, due to its hyperbolic nature, both its mathematical analysis and numerical simulation remain intricate. While the shallow water/Saint-Venant system is capable of addressing a wide range of physical problems, the validity of the approximations leading to the shallow water model becomes questionable when considering density-stratified flows, large friction coefficients, or non-negligible vertical acceleration (Bristeau et al., 2015).

Considering approximations of the underlying real turbulent flow is common practice in geophysical modeling, yielding a wide variety of models. These models are not necessarily fully nested; some, for instance, are singular limits of others. However, within certain parameter ranges, these approximations (and thus models) are fully valid and lead to accurate numerical solutions. In other situations, however, they are associated with significant uncertainties that must be quantified if one intends to use them for real-world applications.

The quantification of those uncertainties in geophysical models is a difficult topic yet crucial in many applications such as data assimilation, or parameters calibration. The error associated to models and their proper dynamics have been most often empirically modelled through additive random forcing, or random perturbation of their parameters. For several years there is a strong interest in proposing stochastic models with so-called transport noise. There are both theoretical and practical motivations supporting such models. Questions revolving around the issue of regularization by noise, initiated by F. Flandoli's work (Flandoli, 2011), as well as questions on turbulence representation by stochastic process is at the heart of many theoretical studies (Brzeżniak et al., 1991; Debussche et al., 2023; Flandoli and Pappalettera, 2021; Galeati and Luo, 2023; Lang et al., 2023a; Majda et al., 1999). In this work we will focus on a Newtonian methodological framework derived from stochastic transport: the modelling under location uncertainty (LU) (Mémin, 2014). This setting enables to derive stochastic large-scale representation of fluid flows from physical conservation principles in the same way as their deterministic counterparts. It leads to energy conservation property by a natural fluctuation-dissipation equilibrium between the energy brought by the noise and the one dissipated by a noise-induced diffusion term, akin to a generalized Boussinesq Reynolds stress model type, that is imposed by the theoretical derivation. The LU framework has been applied to many configurations ranging from idealized simple toy models (Bauer et al., 2020a,b; Brecht et al., 2021; Chapron et al., 2018; Li et al., 2023) to up-to-date models of computational fluid dynamics (Chandramouli et al., 2018, 2020; Kadri Harouna and Mémin, 2017; Tucciarone et al., 2025). This modelling setting has been used also for physical analysis (Pinier et al.,

2019; Tissot et al., 2021, 2023) and data assimilation (Chandramouli et al., 2020; Dufée et al., 2022, 2023; Yang and Mémin, 2019).

Numerically, several different schemes have been proposed to implement these type of models. The crucial point is to ensure a proper balance between the energy brought by the noise and the associated diffusion term. This balance ensures energy conservation at the level of the continuous equations. However, at the discrete level, achieving this equilibrium between the transport noise and its associated diffusion is not straightforward to guarantee. Additionally, considering higher-order temporal discretizations than Euler schemes in a stochastic setting presents the difficult task of sampling the so-called Lévy area, which is generally very costly (Foster et al., 2020). In a recent study, we have shown that neglecting such terms may indeed be beneficial for the stochastic simulation of LU models (Boulvard and Mémin, 2024; Fiorini et al., 2023). This leads to very simple discrete schemes that closely resemble their deterministic counterparts.

In this work, our focus will be on deriving efficient discrete schemes for a stochastic version of the shallow water model as derived and analyzed in (Brecht et al., 2021; Lang et al., 2023a). Specifically, our approach departs from that of (Brecht et al., 2021; Lang et al., 2023a) by introducing new, time-wise "second-order?" methods – the precise meaning of which will be clarified below. These schemes, based on an iterated double advection of the noise, enable an implicit implementation of the noise-associated diffusion, thereby allowing for a conservative formulation and, consequently, a natural finite-volume integration. This ensures, at the discrete level, the natural continuous fluctuation-dissipation balance discussed above. The resulting scheme extends entropy stable methods previously proposed in the discrete setting (El Hassanieh et al., 2024).

In this work we focus principally on the numerical analysis of the schemes proposed. To keep things tractable we focus on the Saint-Venant equations, with a numerical validation for both idealistic and realistic configurations. The numerical schemes proposed can be readily extended to others models. They have been for instance successfully implemented in a realistic circulation model based on the hydrostatic primitive equations (Tucciarone et al., 2025) or for multilayer quasi-geostrophic models (Clement et al., 2025; Fiorini et al., 2022; Li et al., 2023).

The paper is organized as follow. In a first section we start by a general description of the modelling under location uncertainty, introducing the key concepts and theoretical foundations with a particular focus on the shallow-water equations. We then move on to a detailed discussion of the semi-discrete formulation, where we focus on developing a framework that leads to an implicit diffusion mechanism through a double advection process. The next section, Section 4, is dedicated to the discretization process, where we outline the numerical methods employed to translate the continuous stochastic model into a discrete format suitable for computational implementation. This section details the specific schemes used and discusses their properties, including stability and accuracy. In Section 5, we describe the algorithmic implementation of the proposed schemes. Finally, in Section 6, we present the outcomes of our numerical experiments on both an idealistic test case and a realistic configuration for

which real-world data are available. In both cases ensemble of realizations are simulated and compared to either to ground truth defined from deterministic simulation at higher resolution in the idealistic case or to real-world observation in the realistic case. Then, in the appendix, we delve further into the interpretations of the double advection process, through the discretization of the Itô-Wentzell formulae and then through its relation with Milstein schemes.

2 Location uncertainty and Saint-Venant equations

In the modelling under location uncertainty (LU) formalism, the fluid flow map, X, over the bounded domain $\mathcal{S} \subset \mathbb{R}^3$ is represented by the following semi-martingale form:

$$\mathrm{d}X_t = u(X_t, t)\mathrm{d}t + \sigma_t(X_t)\mathrm{d}B_t. \tag{1}$$

The first component, $u(X_t, t)$, of this decomposition corresponds to a smoothly varying component of the (Lagrangian) velocity of the flow. It is correlated both in space and time and is associated with the integration of the equations of motion. The second component, $\sigma_t(X_t)\mathrm{d}B_t$, represents a stochastic contribution, often referred to as noise. This component captures processes that cannot be resolved at a prescribed resolution or have been neglected through numerical or physical modeling approximations. The noise component is a function-valued stochastic process defined from a cylindrical Wiener process B on $L^2(\mathcal{S}, \mathbb{R}^d)$, the space of square integrable functions on $\mathcal{S}$ with values in $\mathbb{R}^d$,

$$B = \sum_{\kappa=0}^{\infty} \hat{\beta}^\kappa e_\kappa,$$

where $(e_\kappa)_{\kappa\in\mathbb{N}}$ is an orthonormal basis of $L^2(\mathcal{S}, \mathbb{R}^d)$ and $(\hat{\beta}_\kappa)_{\kappa\in\mathbb{N}}$ is a sequence of independent standard Brownian motions on a stochastic basis $(\Omega, \mathcal{F}, (\mathcal{F}_t)_{t\in[0,T]}, \mathbb{P})$ (Prato and Zabczyk, 1992). To ensure convergence of the series above, the spatial structure of the noise is specified through a (time dependent) Hilbert-Schmidt integral correlation operator, σ_t, mapping $L^2(\mathcal{S}, \mathbb{R}^d)$ into itself and defined from a bounded and symmetric kernel $\widehat{\sigma}$:

$$\sigma_t(x)f \;:=\; \int_{\mathcal{S}} \widehat{\sigma}(x, y, t)\; f(y)\; \mathrm{d}y,\; f \in L^2(\mathcal{S}, \mathbb{R}^d),$$

where for each (x, y, t), $\widehat{\sigma}(x, y, t)$ is a $d \times d$ symmetric[1] tensor bounded in x, y and t. The noise is finally written as the Wiener process:

$$\sigma_t B_t = \sum_{\kappa=0}^{\infty} \hat{\beta}_t^\kappa \sigma_t e_\kappa,$$

[1]There is no loss of generality in imposing this symmetry, since a Gaussian noise with a non-symmetric correlation tensor yields a positive-definite covariance operator, that can equivalently be represented as the product of symmetric square-roots correlation operators.

where the series converges in $L^2(\mathcal{S}, \mathbb{R}^d)$ almost surely and in $L^p(\Omega)$ for all $p \in \mathbb{N}$ and equation (1) should be understood in the Itô sense. To avoid, any confusion, we may further write the dependence of the Wiener process in terms of the other variables:

$$\sigma_t B_t(x, \omega) = \sum_{\kappa \in \mathbb{N}} \hat{\beta}_t^\kappa(\omega) \sigma_t e_\kappa(x),$$

with ω denoting the random parameter. Let us note, that in this work the correlation operator is assumed to be deterministic. However, it could perfectly depends on randomness. In that case, a stochastic integrability assumption must be assumed (Debussche et al., 2024b; Li et al., 2023).

As the covariance operator is self-adjoint and compact, there exists $(\phi_\kappa(t))_\kappa$ a complete orthogonal system composed of the correlation operator eigenfunctions at each time $t \in \mathbb{R}$. It can be shown that there exists another sequence of independent standard Brownian motions, on the same stochastic basis $(\Omega, \mathcal{F}, (\mathcal{F}_t)_{t\in[0,T]}, \mathbb{P})$ with the representation:

$$\sigma_t \, B_t = \sum_{\kappa=0}^{\infty} \phi_\kappa(t) \, \beta_t^\kappa. \tag{2}$$

This Gaussian random field is associated to the two-times, two-points covariance tensor given by

$$Q(x, y, t, t') = \mathbb{E}\big(\sigma_t \, \mathrm{d}W_t(x) \; \sigma_{t'} \, \mathrm{d}W_{t'}(y)\big) = \int_{\mathcal{S}} \widehat{\sigma}(x, z, t) \, \widehat{\sigma}(z, y, t') \mathrm{d}y \, \delta(t - t') \mathrm{d}t \, ,$$

with the diagonal part (i.e. the one-time auto-correlation), referred to, in the following, as the variance tensor, and denoted by

$$a_t(x) = \int_{\mathcal{S}} \widehat{\sigma}(x, y, t) \, \widehat{\sigma}(y, x, t) \; = \; \sum_{\kappa=0}^{\infty} \phi_\kappa(x, t) \, \phi_\kappa^T(x, t). \tag{3}$$

The variance tensor, which has the dimension of a viscosity in $m^2 s^{-1}$, plays a central role in the LU representation and is associated to the noise quadratic variation, whose definition and properties are briefly recalled in the appendix.

2.1 Scalar conservation law

The goal of this section is to provide an Eulerian form of the material derivative in a stochastic setting. We start by deriving conservation relations for a stochastic scalar variable. We first consider $\theta_t(x)$ a stochastic Eulerian scalar variable, with the corresponding Lagrangian variable denoted $\theta_t(X_t)$. Both descriptions of the variable are classically linked by a total variation formula (TVF) which describes their respective evolutions. We now undertake the writing of this formula. As $\theta_t(X_t) = \theta(X_t(\omega), t, \omega)$ is necessarily defined through the composition of two stochastic processes (Mémin, 2014), we cannot use the classical Itô formula, which applies only to deterministic functions, to compute its differential.

Instead, we must apply a generalized version amenable to the composition of two processes, referred to as the Itô-Wentzell formula (Kunita, 1990) to get our total variation formula:

$$\mathrm{d}\theta_t(X_t) = \mathrm{d}_t\theta_t(X_t) + (\mathrm{d}X_t \cdot \nabla)\theta_t(X_t) + \frac{1}{2}\frac{\partial^2}{\partial x^2}\theta_t(X_t) : \mathrm{d}\Big\langle X \Big\rangle_t + \sum_{i=1}^{d} \mathrm{d}\Big\langle \frac{\partial}{\partial x_i}\theta(X), X^i \Big\rangle_t, \tag{TVF}$$

where

$$A : B := \sum_{i,j=1}^{d} A_{i,j}B_{i,j},$$

denotes the Hadamard product and where $\big\langle X, Y \big\rangle_t$ and $\big\langle X \big\rangle_t = \big\langle X, X \big\rangle_t$ denote the quadratic covariation and variation, respectively. The definitions of these processes as well as their main properties are briefly summarized in the appendix for the reader's convenience.

Now the conservation of variable $\theta_t(X_t)$ spells out in Lagrangian form as:

$$\theta_t(X_t) = \theta_t(X_t)\big|_{t=0} \quad \text{which implies} \quad \mathrm{d}\theta_t(X_t) = 0, \tag{4}$$

and thanks to our total variation formula (TVF) it can also be expressed in Eulerian formalism:

$$\mathrm{d}_t\theta_t = -(\mathrm{d}X_t \cdot \nabla)\theta_t(X_t) - \frac{1}{2}\frac{\partial^2}{\partial x^2}\theta_t(X_t) : \mathrm{d}\Big\langle X \Big\rangle_t - \sum_{i=1}^{d} \mathrm{d}\Big\langle \frac{\partial}{\partial x_i}\theta(X), X^i \Big\rangle_t. \tag{5}$$

This first expression is, however, implicit in θ since the expression

$$\mathrm{d}\Big\langle \frac{\partial}{\partial x_i}\theta(X), X^i \Big\rangle_t,$$

is usually unknown. For a deterministic function this latter quadratic variation term cancels out and we recover the classical Itô formula. For a transported quantity it is possible to obtain an explicit expression of the Itô-Wentzell quadratic term by reiterating (5) with the injection of the martingale part of the left-hand side of (5) – i.e. $-(\sigma \mathrm{d}B_t \cdot \nabla)\theta$ – in $\mathrm{d}\big\langle \frac{\partial}{\partial x_i}\theta(X), X^i \big\rangle_t$ as only the martingale components are involved in the quadratic covariations expression (51). With some algebra this yields the stochastic material derivative:

$$\mathbb{D}_t\theta_t = \mathrm{d}_t\theta_t + \Big(\big((u - u^*)\mathrm{d}t + \sigma_t \mathrm{d}B_t\big) \cdot \nabla\Big)\theta_t - \frac{1}{2}\nabla \cdot (a_t \nabla\theta_t)\mathrm{d}t, \tag{6}$$

where a_t is the variance tensor (3), formally reads $(\sigma_t \cdot \sigma_t^T)$ and $u^* := \frac{1}{2}\nabla \cdot a_t - \sigma_t^T(\nabla \cdot \sigma_t)$.

Remark 1. *The previous procedure can be indeed interpreted as a total reinjection of the full advection* (5) *into the Ito-Wentzell quadratic variation term as only the martingale part leads to non zero quadratic variation. The fact that the stochastic material derivative can be thought of as a double iteration of advection operator will be pushed forward in the following for the constitution and the justification of discrete numerical schemes.*

So far, all the stochastic integrals have been interpreted in terms of Itô integrals. It is possible (for smooth enough integrand) to safely move to a Stratonovich integral representation (see B, where transformation between the two integrals are recalled). This latter has the advantage to be associated with the classical chain rule, but looses the martingale property of the Itô integral: its expectation is not anymore zero.

Using this conversion rule the Stratonovich representation of the LU stochastic form (1) reads (cf. (Bauer et al., 2020a)):

$$\mathrm{d}X_t = \Big(u - \frac{1}{2}\nabla\cdot a_t + \frac{1}{2}\sigma_t^T(\nabla\cdot\sigma_t)\Big)\mathrm{d}t + \sigma_t \circ \mathrm{d}B_t. \tag{7}$$

For a transported random tracer θ (which is assumed to be smoother than in the Itô setting – namely C^3 in space and C^2 in time) advected by a Stratonovich flow, the generalized Itô's formula (Kunita, 1990) has the form of a classical Lagrangian derivative (with Einstein summation convention of repeated indices):

$$\mathrm{d}\theta_t(X_t) = \mathrm{d}_t\circ\,\theta_t(X_t) + \frac{\partial\theta}{\partial x_i}(X_t)\circ\mathrm{d}X_t^i, \tag{8}$$

where $\mathrm{d}_t\circ\,\theta_t(x) \triangleq \theta(x,t+\frac{\mathrm{d}t}{2})-\theta(x,t-\frac{\mathrm{d}t}{2})$ stands for the centered time increment. Substituting (7) in (8), we deduce a Stratonovich representation of the stochastic transport operator

Corollary 1. *Using the Stratonovich notation we get the following formula for the stochastic material derivative (cf (Bauer et al., 2020a)):*

$$\mathbb{D}_t\circ : \theta_t \mapsto \mathrm{d}_t\circ\,\theta_t + \Big(\big((u-u^\circ)\mathrm{d}t + \sigma_t\circ\mathrm{d}B_t\big)\cdot\nabla\Big)\theta_t, \tag{9}$$

with $u^\circ = u^* + \frac{1}{2}(\sigma_t^T\,\nabla\cdot\sigma_t)$.

The combination of the transport operator with a stochastic representation of the Reynolds transport theorem enables us to formulate a stochastic representation of the Navier-Stokes equations (Mémin, 2014) based on the conventional physical conservation properties.

As demonstrated in (Debussche et al., 2023), the LU Navier-Stokes system admits weak (probabilistic) solutions in 3D (with uniqueness in 2D) and in the limit of vanishing noise, this system converges to the deterministic Navier-Stokes equations, providing a consistency guarantee for the large-scale representation by the stochastic system. This can be seen as analogous to the grid convergence required for reliable large-eddy simulation of the Navier-Stokes equations (Guermond et al., 2004; Smagorinsky, 1963).

From the representation under location uncertainty of the Navier-Stokes equations, any classical geophysical approximations defined by appropriate scaling of the various quantities involved can be performed. However, the noise introduces an additional degree of freedom that must also be properly scaled (Resseguier et al., 2017a,b,c). Different scalings of the noise may yield different stochastic systems (see for instance, (Resseguier et al., 2017b,c) for two

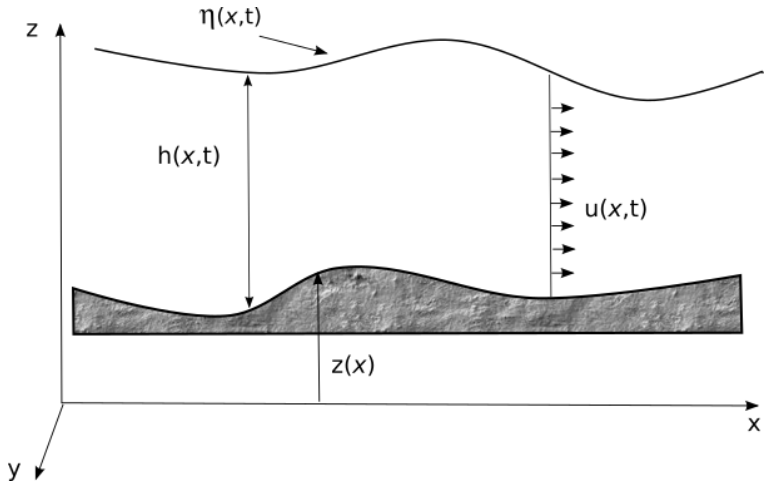

Figure 1: Illustration of a single-layered shallow water system. The water height is denoted h, while η and z represent the altitude of the free surface and bottom topography, respectively. As a result, we have $h = \eta - z$.

different surface quasi-geostrophic models associated with moderate and strong noise, respectively) or systems with additional terms bringing new physical interpretations (see (Pinier et al., 2019) for an example involving turbulent wall model).

In this paper we focus on the stochastic shallow water model. This system has been derived in (Brecht et al., 2021) for a moderate noise scaling. The same system has been theoretically analysed in (Lang et al., 2023b). It has been shown to admit local (in time) pathwise strong solutions.

2.2 Stochastic shallow water model

In a non-rotating setting, the stochastic Saint-Venant system under location uncertainty derived in ((Brecht et al., 2021)) reads:

$$\mathbb{D}_t h + h\nabla \cdot u \mathrm{d}t = 0, \tag{10a}$$

$$\mathbb{D}_t u + g\nabla(h+z)\mathrm{d}t = 0, \tag{10b}$$

$$\nabla \cdot \sigma_t \mathrm{d}B_t = 0 \quad \nabla \cdot u^* = 0, \tag{10c}$$

where $\mathbb{D}_t$ is defined by (6).

In this system $h(x,t)$ is the water height, z denotes the altitude of the lower rigid bottom surface (the sea bed topography for ocean, or the ground topography for atmosphere) and $\eta(x,t) = h + z$ stands for the altitude of the free surface (see fig. 1). The gravitational acceleration constant is denoted g.

Expending the stochastic transport operator we have, in Itô form, the full

system that reads

$$\mathrm{d}_t h + \big((u-u^*)\mathrm{d}t + \sigma_t \mathrm{d}B_t\big)\cdot\nabla h + h\nabla\cdot u\mathrm{d}t - \frac{1}{2}\nabla\cdot(a\nabla h)\mathrm{d}t = 0, \tag{11a}$$

$$\mathrm{d}_t u + \Big(\big((u-u^*)\mathrm{d}t + \sigma_t \mathrm{d}B_t\big)\cdot\nabla\Big)u + g\nabla(h+z)\mathrm{d}t - \frac{1}{2}\nabla\cdot(a\nabla u)\mathrm{d}t = 0, \tag{11b}$$

or in the equivalent Stratonovich form

$$\mathrm{d}_t \circ h + \big((u-u^\circ)\mathrm{d}t + \sigma_t \circ \mathrm{d}B_t\big)\cdot\nabla h + h\nabla\cdot u\mathrm{d}t = 0, \tag{12a}$$

$$\mathrm{d}_t \circ u + \Big(\big((u-u^\circ)\mathrm{d}t + \sigma_t \circ \mathrm{d}B_t\big)\cdot\nabla\Big)u + g\nabla(h+z)\mathrm{d}t = 0. \tag{12b}$$

Remark 2. *The two stochastic representations above closely resemble the deterministic system in their structure. To ease the reading, we will systematically draw parallels between the stochastic setting and the deterministic formulation of the Saint-Venant equations:*

$$\partial_t h + u\cdot\nabla h + h\nabla\cdot u = 0, \tag{13a}$$

$$\partial_t u + (u\cdot\nabla)u + g\nabla(h+z) = 0. \tag{13b}$$

Such a comparison will be particularly relevant as the numerical integration of the stochastic version of the Saint-Venant equation will remain formally close to its deterministic counterpart.

2.3 Saint-Venant equations over the water height flux

We now write the systems for Itô and Stratonovich integrals in flux form, as it is classically done in the deterministic setting.

Formulation 1. *Equations* (11a) *and* (11b) *may be expressed for h and hu in the following fashion:*

$$\mathrm{d}_t h + \big((u-u^*)\mathrm{d}t + \sigma_t \mathrm{d}B_t\big)\cdot\nabla h + h\nabla\cdot u\mathrm{d}t - \frac{1}{2}\nabla\cdot(a\nabla h)\mathrm{d}t = 0, \tag{14a}$$

$$\mathrm{d}_t(hu) + \Big(\big((u-u^*)\mathrm{d}t + \sigma_t \mathrm{d}B_t\big)\cdot\nabla\Big)(hu) + hu(\nabla\cdot u)\mathrm{d}t + g\nabla(h+z)\mathrm{d}t - \frac{1}{2}\nabla\cdot(a\nabla u)\mathrm{d}t = 0. \tag{14b}$$

Corollary 2. *In Stratonovich form,* (14a) *and* (14b) *are rewritten as:*

$$\mathrm{d}_t \circ h + \big((u-u^\circ)\mathrm{d}t + \sigma_t \circ \mathrm{d}B_t\big)\cdot\nabla h + h\nabla\cdot u\mathrm{d}t = 0, \tag{15a}$$

$$\mathrm{d}_t \circ (hu) + \Big(\big((u-u^\circ)\mathrm{d}t + \sigma_t \circ \mathrm{d}B_t\big)\cdot\nabla\Big)(hu) + hu(\nabla\cdot u)\mathrm{d}t + gh\nabla(h+z)\mathrm{d}t = 0. \tag{15b}$$

This flux form formulation can be easily obtained in Stratonovich, remembering that Stratonovich integral obeys the classical Leibniz product rule. The Itô version, is then obtained by moving form Stratonovich to Itô. The corresponding deterministic formulation is recalled in the following remark, and is identical in its form to the Stratonovich formulation.

Remark 3. *Likewise, in the deterministic case, we have the following formulation:*

$$\partial_t h + (u \cdot \nabla)h + h\nabla \cdot u = 0, \tag{16a}$$
$$\partial_t (hu) + (u \cdot \nabla)(hu) + hu(\nabla \cdot u) + gh\nabla(h + z) = 0. \tag{16b}$$

2.4 Conservative form of the Saint-Venant equations

From the previous flux forms, conservative formulations of the Saint-Venant equations in Itô or Stratonovich can be obtained through similar algebraic manipulations :

Formulation 2 (Conservative formulation)**.** *System* (14) *is equivalent to the following one:*

$$\mathrm{d}_t h + \nabla \cdot \Big(\big((u - u^*)\mathrm{d}t + \sigma_t \mathrm{d}B_t\big)h \Big) - \frac{1}{2}\nabla \cdot (a\nabla h)\mathrm{d}t = 0, \tag{17a}$$

$$\mathrm{d}_t (hu) + \nabla \cdot \Big(\big((u - u^*)\mathrm{d}t + \sigma_t \mathrm{d}B_t\big) \otimes hu \Big) + \nabla(g\frac{h^2}{2})\mathrm{d}t - \frac{1}{2}\nabla \cdot (a\nabla hu)\mathrm{d}t = -gh\nabla z \mathrm{d}t. \tag{17b}$$

Corollary 3. *System* (17a), (17b) *has the following Stratonovich formulation:*

$$\mathrm{d}_t \circ h + \nabla \cdot \Big(\big((u - u^\circ)\mathrm{d}t + \sigma_t \circ \mathrm{d}B_t\big)h \Big) = 0, \tag{18a}$$

and

$$\mathrm{d}_t \circ hu + \nabla \cdot \Big(\big((u - u^\circ)\mathrm{d}t + \sigma_t \circ \mathrm{d}B_t\big) \otimes hu \Big) + \nabla(g\frac{h^2}{2})\mathrm{d}t = -gh\nabla z \mathrm{d}t. \tag{18b}$$

For reader's convenience the deterministic formulation is provided in the following remark.

Remark 4. *The deterministic equivalent to formulae* (17) *and* (18) *is*

$$\partial_t h + \nabla \cdot (uh) = 0, \tag{19a}$$

and

$$\partial_t hu + \nabla \cdot (u \otimes hu) + \nabla(g\frac{h^2}{2}) = -gh\nabla z. \tag{19b}$$

2.5 Compact notations for Saint-Venant equations

In order to simplifiy the exposition, we now introduce a more concise presentation of the Saint-Venant equations. When comparing the Saint-Venant equations in Itô form, Stratonovich notation, and in the deterministic case, a notable distinction is the inclusion of a modified advection term in the convective term. To address this, we will isolate the advection term in the vector formulation of our Saint-Venant-LU equations.

Definition 1. State vector *We name:*

$$U := \begin{pmatrix} h \\ hu \end{pmatrix},$$

the state vector.

We further define an infinitesimal advection generating the flux:

Definition 2. *For $\alpha^{\mathrm{d}t,\mathrm{d}B_t}$ a given semi-martingale advection, we set:*

$$f[\alpha^{\mathrm{d}t,\mathrm{d}B_t}](U) := \left(\alpha^{\mathrm{d}t,\mathrm{d}B_t} \cdot \nabla\right) U + \begin{pmatrix} 0 & 0 \\ g\mathrm{d}t\nabla & 0 \end{pmatrix} U,$$

the advection operator deriving from the flow:

$$F[\alpha^{\mathrm{d}t,\mathrm{d}B_t}](U) := \alpha^{\mathrm{d}t,\mathrm{d}B_t} \otimes U + \begin{pmatrix} 0 \\ g\mathrm{d}t\frac{h^2}{2} \end{pmatrix}.$$

With these tools, the Saint-Venant equations may be expressed in compact form as:

Formulation 3 (Vectorized Saint-Venant equations under Ito notation)**.** *We have the following equivalent form*

$$(14) \iff \mathrm{d}_t U + f\left[\left((u-u^*)\mathrm{d}t + \sigma_t \mathrm{d}B_t\right)\right](U) - \frac{1}{2}\nabla\cdot(a\nabla U)\mathrm{d}t = 0, \tag{20}$$

$$(17) \iff \mathrm{d}_t U + \nabla\cdot F\left[\left((u-u^*)\mathrm{d}t + \sigma_t \mathrm{d}B_t\right)\right](U) - \frac{1}{2}\nabla\cdot(a\nabla U)\mathrm{d}t = 0. \tag{21}$$

Formulation 4 (Vectorized Saint-Venant equations under Stratonovich notation)**.** *We have the equivalent form*

$$(15) \iff \partial_t U + f\left[\left((u-u^\circ)\mathrm{d}t + \sigma \mathrm{d}B_t\right)\right](U) = 0, \tag{22}$$

$$(18) \iff \mathrm{d}_t U + \nabla\cdot F\left[\left((u-u^\circ)\mathrm{d}t + \sigma_t \mathrm{d}B_t\right)\right](U). \tag{23}$$

In the deterministic case, these compact formulations reads:

Formulation 5 (Vectorized deterministic Saint-Venant equations)**.** *We have the following equivalent form*

$$(16) \iff \partial_t U + f[u](U) = 0, \tag{24}$$

$$(19) \iff \partial_t U + \nabla\cdot F[u](U) = 0. \tag{25}$$

3 Semi-discrete formulation: toward an implicit diffusion

The main goal of our computations below is to find a consistent time-wise discretization of our Saint-Venant equation with implicit diffusion, using what we call a "double advection". As the stochastic Saint-Venant equations derives from the formulation of the stochastic material derivative we will mostly focus on the later.

3.1 Formulation of the stochastic transport operator through a double advection

When compared with its "standard" deterministic counterpart, the stochastic material derivative has two additional terms originating from Itô-Wentzell formula:

$$(-u^*\mathrm{d}t\cdot\nabla)\theta \quad \text{and} \quad -\frac{1}{2}\nabla\cdot(a\nabla\theta)\mathrm{d}t. \tag{26}$$

As explained in section 2, those additional terms are related to comparable supplementary quadratic variation and cross variation components in (5) i.e

$$\frac{1}{2}\frac{\partial^2}{\partial x^2}\theta_t(X_t) : \mathrm{d}\Big\langle X\Big\rangle_t, \qquad (\textbf{quadratic term})$$

$$\sum_{i=1}^{d}\mathrm{d}\Big\langle\frac{\partial}{\partial x_i}\theta(X), X^i\Big\rangle_t. \qquad (\textbf{cross term})$$

Those terms, in turn have their roots in the Itô-Wentzell formulae at the discrete level. Our goal in the next section is to reformulate this mechanism so as to introduce the following term:

$$\big(\sigma^T\cdot\nabla\big)\big((\sigma^T\cdot\nabla)\theta_t\big)\mathrm{d}t. \qquad (\textbf{double advection})$$

Beforehand, we introduce the following second-order component:

$$a : \frac{\partial^2}{\partial x^2}\theta_t. \qquad (\textbf{diffusion term})$$

This (**diffusion term**) naturally springs up from the expansion of (**quadratic term**) and (**cross term**) as we will show now.

Lemma 1. *The* (**quadratic term**) *and* (**cross term**) *can be expanded as:*

$$\frac{1}{2}\frac{\partial^2}{\partial x^2}\theta(t,X_t) : \mathrm{d}\big\langle X\big\rangle_t = \frac{1}{2}a : \frac{\partial^2}{\partial x^2}\theta_t\mathrm{d}t,$$

$$\sum_{i=1}^{d}\mathrm{d}\Big\langle\frac{\partial}{\partial x_i}\theta_\cdot(X), X_i\Big\rangle_t = -\big((\sigma_t^T\,\nabla\cdot\sigma_t)\cdot\nabla\big)\theta_t\mathrm{d}t - a : \frac{\partial^2}{\partial x^2}\theta_t\mathrm{d}t.$$

Proof. The first result is justified upon directly computing the quadratic variation of X_t, while the second derives from the conservation of θ, (5) which we recall here:

$$\mathrm{d}_t\theta_t = -(\mathrm{d}X_t \cdot \nabla)\theta_t(X_t) - \frac{1}{2}\frac{\partial^2}{\partial x^2}\theta_t(X_t) : \mathrm{d}\Big\langle X \Big\rangle_t - \sum_{i=1}^{d} \mathrm{d}\Big\langle \frac{\partial}{\partial x_i}\theta(X), X^i \Big\rangle_t .$$

□

Remark 5. *The computations in this section will be conducted within a broader framework than the LU Saint-Venant model considered here. Specifically, we will not impose condition* (10c)*:*

$$\nabla \cdot \sigma_t \mathrm{d}B_t = 0 \quad \nabla \cdot u^* = 0.$$

Under this relaxed hypothesis we can formulate more general LU wave models such as (Debussche et al., 2024a)

In the following sections we will show that the (**double advection**) also generates the (**diffusion term**), which is, in turn, a key component of expression (26). We begin by establishing the framework for our computations.

3.2 Regularity requirements

Let us recall the regularity requirements verified by θ_t and X_t and which are necessary in the Ito-Wentzell formula's framework, as expressed in (Kunita, 1990):

Definition 3 (Regularity requirements over the functional θ_t.)**.** *We consider that $\theta_t(x)$ defined over $[0,T] \times \mathbb{R}^d$ verifies that:*

1. *$\theta_t(x)$ is twice continuously differentiable in x.*
2. *For all x, $\theta_t(x)$ is a continuous semi-martingale, where:*
   (a) *$\theta_t(x) = \phi^0(x) + \sum_{\kappa=1}^{m} \int_0^t \phi_s^\kappa(x) d\beta_s^\kappa$ for all $x \in \mathbb{R}^d$, a.s, the β_s^κ being standard Brownian motions, the ϕ_s^κ being continuous random fields in $x \in \mathbb{R}^d$ and $s \in [0,T]$ satisfying:*
      i. *$\phi_s^\kappa(x)$ are twice continuously differentiable in x,*
      ii. *for each x, $\phi_s^\kappa(x)$ are adapted processes.*

For the Itô-Wentzell formula there is further the requirement that X_t be a time-continuous semi-martingale. However in view of relation (5) and especially of the (**cross term**) it is apparent that we need further regularity conditions for the field $X_t : \mathcal{S} \mapsto \mathbb{R}^d$:

Definition 4 (Regularity requirements over X_t)**.** *The continuous semi-martingale* X_t*:*

$$dX_t = u(t, X_t)\mathrm{d}t + \sigma_t(X_t)\mathrm{d}B_t,$$

is such that:

1. *σ is continuous in time and $\sigma(t, \cdot)$ is a kernel Hilbert-Schmidt operator with kernel $C^1(\mathbb{R}^d, \mathbb{R}^d)$,*
2. *u is continuous in time with $u(t, \cdot) \in C^1(\mathbb{R}^d)$.*

3.3 Formal link

Now, our main goal is to prove by the way of the (**diffusion term**) the following link between the (**double advection**) and the components of the stochastic material derivative:

Proposition 1. *The* (**double advection**) *generates the components of* (26) *in the following way:*

$$\lim_{n\to\infty} -\frac{1}{2}\sum_{k=0}^{n-1}\big(\sigma\Delta B_{t_k}\cdot\nabla\big)\big((\sigma\Delta B_{t_k}\cdot\nabla)\theta_{t_k}\big) - \int_0^T\big((u^* - u^\dagger)\cdot\nabla\big)\theta_t\mathrm{d}t$$
$$= -\int_0^T \frac{1}{2}\nabla\cdot(a\nabla\theta_t)\mathrm{d}t - \int_0^T (u^*\cdot\nabla)\theta_t\mathrm{d}t,$$

with $u^\dagger = -\frac{1}{2}\big(\sigma^T(\nabla\cdot\sigma)\big)^T$.

The proof of this Proposition is articulated as follows: first we will verify that the left-hand term in Proposition 1 is indeed the double advection, then prove the relation between the (**double advection**) and the (**diffusion term**), and finally we will show how the former generates the components of (26).

3.3.1 Convergence of the (double advection) to the (diffusion term)

Lemma 2. *Let θ_t and X_t following the requirements of definition 3 and 4 respectively; we have the following limit in probability:*

$$\sum_{k=0}^{n-1}\big(\sigma_{t_k}\Delta B_{t_k}\cdot\nabla\big)\big((\sigma_{t_k}\Delta B_{t_k}\cdot\nabla)\theta_{t_k}\big) \xrightarrow[n\to\infty]{} \int_0^T\big(\sigma_t^T\cdot\nabla\big)\big((\sigma_t^T\cdot\nabla)\theta_t\big)\mathrm{d}t.$$

Proof.

$$\sum_{k=0}^{n-1}\big(\sigma\Delta B_{t_k}\cdot\nabla\big)\big((\sigma\Delta B_{t_k}\cdot\nabla)\theta_{t_k}\big)=\sum_{k=0}^{n-1}\sum_{i,j,l,m=1}^{d}\big(\sigma_{i,j}\Delta B^j_{t_k}\frac{\partial}{\partial x^i}\big)\big((\sigma_{l,m}\Delta B^m_{t_k}\frac{\partial}{\partial x^l})\theta_{t_k}\big) \tag{27}$$

$$=\sum_{k=0}^{n-1}\sum_{i,j,l,m=1}^{d}\big(\sigma_{i,j}\frac{\partial}{\partial x^i}\big)\big((\sigma_{l,m}\frac{\partial}{\partial x^l})\theta_{t_k}\big)\Delta B^j_{t_k}\Delta B^m_{t_k} \tag{28}$$

$$\xrightarrow[n\to\infty]{}\int_0^T\sum_{i,j,l,m=1}^{d}\big(\sigma_{i,j}\frac{\partial}{\partial x^i}\big)\big((\sigma_{l,m}\frac{\partial}{\partial x^l})\theta_t\big)\mathrm{d}\Big\langle B^j,B^m\Big\rangle_t \tag{29}$$

$$=\int_0^T\sum_{i,j,l=1}^{d}\big(\sigma_{i,j}\frac{\partial}{\partial x^i}\big)\big((\sigma_{l,j}\frac{\partial}{\partial x^l})\theta_t\big)\mathrm{d}t \tag{30}$$

$$=\int_0^T\big(\sigma^T\cdot\nabla\big)\big((\sigma^T\cdot\nabla)\theta_t\big)\mathrm{d}t. \tag{31}$$

□

The following result establishes a link between the **double advection** and the **diffusion term**

Lemma 3 (Link between **double advection** and the **diffusion term**)**.** *The* ***double advection*** *is related to the* ***diffusion term*** *in the following way:*

$$\big(\sigma^T\cdot\nabla\big)\big((\sigma^T\cdot\nabla)\theta_t\big)=\bigg(\Big((\nabla\cdot a)-\big(\sigma^T(\nabla\cdot\sigma)\big)^T\Big)\cdot\nabla\bigg)\theta_t+a:\frac{\partial^2}{\partial x^2}\theta_t$$

Proof. One has

$$\sum_{i,j,l=1}^{d}\big(\sigma_{i,j}\frac{\partial}{\partial x^i}\big)\big((\sigma_{l,j}\frac{\partial}{\partial x^l})\theta_t\big)=\sum_{i,j,l=1}^{d}\big(\sigma_{i,j}(\frac{\partial}{\partial x^i}\sigma_{l,j})\frac{\partial}{\partial x^l}\big)\theta_t+\sigma_{i,j}\sigma_{l,j}\frac{\partial^2}{\partial x^i\partial x^l}\theta_t$$

i.e

$$\big(\sigma^T\cdot\nabla\big)\big((\sigma^T\cdot\nabla)\theta_t\big)=\big((\sigma:\nabla\sigma^T)\cdot\nabla\big)\theta_t+a:\frac{\partial^2}{\partial x^2}\theta_t$$

Moreover

$$\sum_{i,j,l=1}^{d}\big(\sigma_{i,j}(\frac{\partial}{\partial x^i}\sigma_{l,j})\frac{\partial}{\partial x^l}\big)\theta_t=\sum_{i,j,l=1}^{d}\Big(\big(\frac{\partial}{\partial x^i}(\sigma_{i,j}\sigma_{l,j})-(\frac{\partial}{\partial x^i}\sigma_{i,j})\sigma_{l,j}\big)\frac{\partial}{\partial x^l}\Big)\theta_t$$

i.e

$$\big((\sigma:\nabla\sigma^T)\cdot\nabla\big)\theta_t=\bigg(\Big((\nabla\cdot a)-\big(\sigma^T(\nabla\cdot\sigma)\big)^T\Big)\cdot\nabla\bigg)\theta_t$$

□

Those two results are now summed up in the following result:

Lemma 4.

$$\lim_{n\to\infty}\sum_{k=0}^{n-1}\big(\sigma\Delta B_{t_k}\cdot\nabla\big)\big((\sigma\Delta B_{t_k}\cdot\nabla)\theta_{t_k}\big)=\int_0^T a:\frac{\partial^2}{\partial x^2}\theta_t\mathrm{d}t+\int_0^T\bigg(\Big((\nabla\cdot a)-\big(\sigma^T(\nabla\cdot\sigma)\big)^T\Big)\cdot\nabla\bigg)\theta_t\mathrm{d}t \tag{32}$$

3.3.2 Relation between the (diffusion term) and the components of (26)

We now add a Lemma allowing us to reformulate the (**diffusion term**) using components from (26):

Lemma 5.

$$a:\frac{\partial^2}{\partial x^2}\theta_t=\nabla\cdot(a\nabla\theta_t)-\big((\nabla\cdot a)\cdot\nabla\big)\theta_t$$

This relation arises from an immediate product rule. By including Lemma 5 into Lemma 4, we establish a link between the "classical" and "double-advection" constructions of the stochastic material derivative:

Lemma 6.

$$\lim_{n\to\infty}\sum_{k=0}^{n-1}\big(\sigma\Delta B_{t_k}\cdot\nabla\big)\big((\sigma\Delta B_{t_k}\cdot\nabla)\theta_{t_k}\big)=\int_0^T\nabla\cdot(a\nabla\theta_t)\mathrm{d}t-\int_0^T\bigg(\Big(\big(\sigma^T(\nabla\cdot\sigma)\big)^T\Big)\cdot\nabla\bigg)\theta_t\mathrm{d}t \tag{33}$$

This last result entails that

$$\lim_{n\to\infty}-\frac{1}{2}\sum_{k=0}^{n-1}\big(\sigma\Delta B_{t_k}\cdot\nabla\big)\big((\sigma\Delta B_{t_k}\cdot\nabla)\theta_{t_k}\big)=-\int_0^T\frac{1}{2}\nabla\cdot(a\nabla\theta_t)\mathrm{d}t+\int_0^T\frac{1}{2}\bigg(\Big(\big(\sigma^T(\nabla\cdot\sigma)\big)^T\Big)\cdot\nabla\bigg)\theta_t\mathrm{d}t.$$

Now that we see how to generate the (**diffusion term**), we may add the modified advection term; recalling that

$$u^*=\frac{1}{2}\nabla\cdot a-\big(\sigma^T(\nabla\cdot\sigma)\big)^T,\quad u^\dagger=-\frac{1}{2}\big(\sigma^T(\nabla\cdot\sigma)\big)^T,$$

we obtain

$$\begin{aligned}\lim_{n\to\infty}-\frac{1}{2}\sum_{k=0}^{n-1}\big(\sigma\Delta B_{t_k}\cdot\nabla\big)\big((\sigma\Delta B_{t_k}\cdot\nabla)\theta_{t_k}\big)-\int_0^T\big((u^*-u^\dagger)\cdot\nabla\big)\theta_t\mathrm{d}t&\\ =-\int_0^T\frac{1}{2}\nabla\cdot(a\nabla\theta_t)\mathrm{d}t-\int_0^T(u^*\cdot\nabla)\theta_t\mathrm{d}t,&\end{aligned}$$

hence our result.

In C, we provide two alternative proofs of this result, each allowing for different interpretations of the underlying mechanisms. The first one is a **modified**

Taylor formula interpretation, which focuses on the Taylor expansion at the root of our total variation formula (TVF) and consequently of the stochastic material derivative (6). By using an alternative remainder for the Taylor expansion, we naturally obtain a (**double advection**) plus an additionnal term that converges to a **modified advection**.

The second interpretation, **Milstein interpretation**, is based on the Milstein scheme – a second order stochastic schemes involving the Lévy area, a complex geometric process. We demonstrate that the double advection discretization schemes put forward in subsection 3.5 are consistent with a simplified Milstein scheme derived from (20), in which the Lévy area is omited. In (Boulvard and Mémin, 2024) numerical diagnostics for a prototypical geophysical flow suggest that this simplification is justifiable when large-scale velocity fluctuations are idealized as a Wiener process, as is the case in the LU scheme.

Now that we can express the specific components of the stochastic material derivative as a double advection, we will examine the effect of adding terms to this advection to achieve a consistent approximation of the LU Saint-Venant equations.

3.4 Modified first order component

This section presents three results addressing the effects of a modified advection: the first examines the inclusion of the deterministic velocity term $(u-u^*)\mathrm{d}t$ in the advection; the second considers a modification of the time discretization of the variable u; and the third incorporates a bathymetry term into our scheme.

Proposition 2 (Modified advection)**.** *Let α be a continuous time process with values in $C^1(\mathbb{R}^d)$ and θ verifying the conditions of definition 3, then:*

$$\sum_{k=0}^{n-1}\big((\alpha_{t_k}\Delta t_k+\sigma\Delta B_{t_k})\cdot\nabla\big)\theta_{t_k}-\frac{1}{2}\sum_{k=0}^{n-1}\Big((\alpha_{t_k}\Delta t_k+\sigma\Delta B_{t_k})\cdot\nabla\Big)\Big(\big((\alpha_{t_k}\Delta t_k+\sigma\Delta B_{t_k})\cdot\nabla\big)\theta_{t_k}\Big)$$
$$\xrightarrow[n\to\infty]{}\int_0^T\left(\Big[\Big(\alpha_t+\frac{1}{2}\big(\sigma^T(\nabla\cdot\sigma)\big)^T\Big)\mathrm{d}t+\sigma\mathrm{d}B_t\Big]\cdot\nabla\right)\theta_t-\frac{1}{2}\nabla\cdot(a\nabla\theta_t)\mathrm{d}t. \quad (34)$$

Proof. This result is an extension of Lemma 6. Here, we only need to prove the convergence argument corresponding to Lemma 2:

$$\sum_{k=0}^{n-1}\big(\alpha_{t_k}\Delta t_k\cdot\nabla\big)\big((\alpha_{t_k}\Delta t_k\cdot\nabla)\theta_{t_k}\big)\xrightarrow[n\to\infty]{}0,$$
$$\sum_{k=0}^{n-1}\big(\alpha_{t_k}\Delta t_k\cdot\nabla\big)\big((\sigma\Delta B_{t_k}\cdot\nabla)\theta_{t_k}\big)\xrightarrow[n\to\infty]{}0,$$
$$\sum_{k=0}^{n-1}\big(\sigma\Delta B_{t_k}\cdot\nabla\big)\big((\alpha_{t_k}\Delta t_k\cdot\nabla)\theta_{t_k}\big)\xrightarrow[n\to\infty]{}0.$$

Let us suppose, for simplicity's sake that the time division is regular, i.e

$$\Delta t_k = \Delta t \xrightarrow[n\to\infty]{} 0,$$

then for the first term we have

$$\sum_{k=0}^{n-1}\big(\alpha_{t_k}\Delta t_k\cdot\nabla\big)\big((\alpha_{t_k}\Delta t_k\cdot\nabla)\theta_{t_k}\big) = \Delta t\underbrace{\sum_{k=0}^{n-1}(\alpha_{t_k}\cdot\nabla)((\alpha_{t_k}\Delta t_k\cdot\nabla)\theta_{t_k})}_{\substack{\xrightarrow{n\to\infty}\int_0^T(\alpha_t\cdot\nabla)((\alpha_t\cdot\nabla)\theta_t)\mathrm{d}t\\ Riemann\\ integral}}$$

thus the first convergence; the next two follow the same pattern albeit with the Riemann integral being replaced by the Itô integral:

$$\sum_{k=0}^{n-1}\big(\alpha_{t_k}\Delta t_k\cdot\nabla\big)\big((\sigma\Delta B_{t_k}\cdot\nabla)\theta_{t_k}\big) = \Delta t\underbrace{\sum_{k=0}^{n-1}\big(\alpha_{t_k}\cdot\nabla\big)\big((\sigma\Delta B_{t_k}\cdot\nabla)\theta_{t_k}\big)}_{\substack{\xrightarrow{n\to\infty}\int_0^T(\alpha_t\cdot\nabla)((\sigma\mathrm{d}B_t\cdot\nabla)\theta_t)\\ Ito\\ integral}},$$

and

$$\sum_{k=0}^{n-1}\big(\sigma\Delta B_{t_k}\cdot\nabla\big)\big((\alpha_{t_k}\Delta t_k\cdot\nabla)\theta_{t_k}\big) = \Delta t\underbrace{\sum_{k=0}^{n-1}\big(\sigma\Delta B_{t_k}\cdot\nabla\big)\big((\alpha_{t_k}\cdot\nabla)\theta_{t_k}\big)}_{\substack{\xrightarrow{n\to\infty}\int_0^T(\sigma\mathrm{d}B_t\cdot\nabla)((\alpha_t\cdot\nabla)\theta_t)\\ Ito\\ integral}},$$

hence our conclusion. □

This first result will be used to add the following deterministic velocity in the advection:

$$\alpha_\cdot = \big(u-(u^*-u^\dagger)\big),\quad u^*-u^\dagger = \frac{1}{2}\nabla\cdot a - \frac{1}{2}\big(\sigma^T(\nabla\cdot\sigma)\big)^T$$

Namely, we have:

Corollary 4. *The stochastic transport operator can be discretized as:*

$$\begin{aligned}\int_0^T \mathbb{D}_t\theta = \lim_{n\to\infty}\sum_{k=0}^{n-1}\bigg(\Big(\big(u-(u^*-u^\dagger)\big)\Delta t_k+\sigma\Delta B_{t_k}\Big)\cdot\nabla\bigg)\theta_{t_k}\\ -\frac{1}{2}\sum_{k=0}^{n-1}\bigg(\Big(\big(u-(u^*-u^\dagger)\big)\Delta t_k+\sigma\Delta B_{t_k}\Big)\cdot\nabla\bigg)\bigg(\Big(\Big(\big(u-(u^*-u^\dagger)\big)\Delta t_k+\sigma\Delta B_{t_k}\Big)\cdot\nabla\Big)\theta_{t_k}\bigg).\end{aligned} \tag{35}$$

Now that we have shown how to discretize the stochastic transport operator we can write a discretization of the LU Saint Venant equations. To that end we need to add a linear operator that is not an advection:

Proposition 3 (Modified linear term)**.** *Let $\alpha.$ be a continuous time process with values in $C^1(\mathbb{R}^d)$ and θ verifying the conditions of definition 3, then:*

$$\begin{aligned}
&\sum_{k=0}^{n-1} f[\alpha_{t_k}\Delta t_k + \sigma\Delta B_{t_k}](\theta_{t_k}) - \frac{1}{2} f[\alpha_{t_k}\Delta t_k + \sigma\Delta B_{t_k}]\big(f[\alpha_{t_k}\Delta t_k + \sigma\Delta B_{t_k}](\theta_{t_k})\big) \\
&\quad := \sum_{k=0}^{n-1} \left(\alpha_{t_k}\Delta t_k + \sigma\Delta B_{t_k}\cdot\nabla + \begin{pmatrix} 0 & 0 \\ g\Delta t_k\nabla & 0 \end{pmatrix}\right)\theta_{t_k} \\
&\qquad -\frac{1}{2}\sum_{k=0}^{n-1} \left(\alpha_{t_k}\Delta t_k + \sigma\Delta B_{t_k}\cdot\nabla + \begin{pmatrix} 0 & 0 \\ g\Delta t_k\nabla & 0 \end{pmatrix}\right) \times \left(\left(\alpha_{t_k}\Delta t_k + \sigma\Delta B_{t_k}\cdot\nabla + \begin{pmatrix} 0 & 0 \\ g\Delta t_k\nabla & 0 \end{pmatrix}\right)\theta_{t_k}\right) \\
&\xrightarrow[n\to\infty]{} \int_0^T \left(\left(\alpha_t \mathrm{d}t + \frac{1}{2}\left(\sigma^T(\nabla\cdot\sigma)\right)^T \mathrm{d}t + \sigma \mathrm{d}B_t\right)\cdot\nabla + \begin{pmatrix} 0 & 0 \\ g\mathrm{d}t\nabla & 0 \end{pmatrix}\right)\theta_t - \frac{1}{2}\nabla\cdot(a\nabla\theta_t)\mathrm{d}t \\
&\quad = \int_0^T f\left[\alpha_t + \frac{1}{2}\left(\sigma^T(\nabla\cdot\sigma)\right)^T \mathrm{d}t + \sigma\mathrm{d}B_t\right](\theta_t) - \frac{1}{2}\nabla\cdot(a\nabla\theta_t)\mathrm{d}t. \qquad (36)
\end{aligned}$$

The first and last expressions relate to formulation (20), enabling us to construct a complete discretization of the LU Saint-Venant equations. We now modify this result to allow for finer adjustments in our time discretization.

Proposition 4 (Modified advection)**.** *Let*

1. *α be a continuous in time process with values in $C^1(\mathbb{R}^d)$,*
2. *β be a continuous in time mapping with $\beta(t,\cdot) \in C^1(\mathbb{R}^d)$,*
3. *γ be a continuous in time kernel Hilbert-Schmidt operator with kernel in $C^1(\mathbb{R}^d, \mathbb{R}^d)$,*

and θ verifying the conditions of definition 3, then:

$$\begin{aligned}
&\sum_{k=0}^{n-1} f\big[\big(\alpha_{t_k} + \beta\Delta t_k + \gamma\Delta B_{t_k}\big)\Delta t_k + \sigma\Delta B_{t_k}\big](\theta_{t_k}) \\
&-\frac{1}{2}\sum_{k=0}^{n-1} f\big[\big(\alpha_{t_k}+\beta\Delta t_k+\gamma\Delta B_{t_k}\big)\Delta t_k+\sigma\Delta B_{t_k}\big]\Big(f\big[\big(\alpha_{t_k}+\beta\Delta t_k+\gamma\Delta B_{t_k}\big)\Delta t_k+\sigma\Delta B_{t_k}\big](\theta_{t_k})\Big) \\
&\qquad \xrightarrow[n\to\infty]{} \int_0^T f\Big[\Big(\alpha_t + \frac{1}{2}\big(\sigma^T(\nabla\cdot\sigma)\big)^T\Big)\mathrm{d}t + \sigma\mathrm{d}B_t\Big](\theta_t) - \frac{1}{2}\nabla\cdot(a\nabla\theta_t)\mathrm{d}t
\end{aligned} \qquad (37)$$

3.5 Three discretization schemes

Before introducing three semi-discrete (time-wise) schemes, let us make the following remark:

Remark 6. *Our discretizations are similar in their forms to the schemes proposed in (Cotter et al., 2019; Fiorini et al., 2023):*

$$\begin{cases} U^{n+1/3} = U^n - f[(u^n - u^\circ)\Delta t + \sigma\Delta B_t](U^n), \\ U^{n+2/3} = \frac{3}{4}U^n + \frac{1}{4}\big(U^{n+1/3} - f[(u^n - u^\circ)\Delta t + \sigma\Delta B_t](U^{n+1/3})\big), \\ U^{n+1} = \frac{1}{3}U^n + \frac{2}{3}\big(U^{n+2/3} - f[(u^n - u^\circ)\Delta t + \sigma\Delta B_t](U^{n+2/3})\big), \end{cases} \tag{38}$$

This implicit diffusion scheme was the source of inspiration for our developments and an important point for finite-volume analysis. However, In (Cotter et al., 2018) the schemes are derived from considerations on the Stratonovich integral, which is not the case here although there is a common root between the Stratonovich integral calculus and our double advection computations. The scheme (Fiorini et al., 2023) is derived from high-order Milstein schemes. The bridge between the proposed double-advection schemes and the Milstein discretization is further developed in C.

Our first scheme, makes use of Propositions 2 and 3 together and reads, recalling once more the notation (20), as follows:

Definition 5 (Two step scheme)**.**

$$\begin{cases} U^{n+1/2} = U^n - f\big[\big(u^n - (u^* - u^\dagger)\big)\Delta t + \sigma\Delta B_t\big](U^n), \\ U^{n+1} = \frac{1}{2}U^n + \frac{1}{2}\Big(U^{n+1/2} - f\big[\big(u^{n+1/2} - (u^* - u^\dagger)\big)\Delta t + \sigma\Delta B_t\big](U^{n+1/2})\Big). \end{cases} \tag{39}$$

However this scheme would entail a possibly zero CFL so we amend the advection part in $f[\cdot]$ and provide the following scheme:

Definition 6 (Two steps scheme with delayed advection)**.**

$$\begin{cases} U^{n+1/2} = U^n - f\big[\big(u^n - (u^* - u^\dagger)\big)\Delta t + \sigma\Delta B_t\big](U^n), \\ U^{n+1} = \frac{1}{2}U^n + \frac{1}{2}\Big(U^{n+1/2} - f\big[\big(u^n - (u^* - u^\dagger)\big)\Delta t + \sigma\Delta B_t\big](U^{n+1/2})\Big). \end{cases} \tag{40}$$

Proof of consistence. System (40) also reads as

$$\begin{aligned} U^{n+1} =& U^n - f\big[\big(u^n - (u^* - u^\dagger)\big)\Delta t + \sigma\Delta B_t\big](U^n) \\ &+ \frac{1}{2}f\big[\big(u^n - (u^* - u^\dagger)\big)\Delta t + \sigma\Delta B_t\big]\Big(f\big[\big(u^n - (u^* - u^\dagger)\big)\Delta t + \sigma\Delta B_t\big](U^n)\Big), \end{aligned}$$

i.e

$$\begin{aligned} U^{n+1} - U^n + & f\big[\big(u^n - (u^* - u^\dagger)\big)\Delta t + \sigma\Delta B_t\big](U^n) \\ & - \frac{1}{2}f\big[\big(u^n - (u^* - u^\dagger)\big)\Delta t + \sigma\Delta B_t\big]\Big(f\big[\big(u^n - (u^* - u^\dagger)\big)\Delta t + \sigma\Delta B_t\big](U^n)\Big) = 0, \end{aligned}$$

which by virtue of Propositions 3 is consistent with (20). □

Definition 7 (Two step scheme with predicted advection)**.**

$$\begin{cases} \tilde{U}^n = U^n - f\big[\big(u^n - (u^* - u^\dagger)\big)\Delta t + \sigma\Delta B_t\big](U^n), \\ U^{n+1/2} = U^n - f\big[\big(\tilde{u}^n - (u^* - u^\dagger)\big)\Delta t + \sigma\Delta B_t\big](U^n), \\ U^{n+1} = \frac{1}{2}U^n + \frac{1}{2}\Big(U^{n+1/2} - f\big[\big(\tilde{u}^n - (u^* - u^\dagger)\big)\Delta t + \sigma\Delta B_t\big](U^{n+1/2})\Big). \end{cases} \tag{41}$$

Proof of consistence. We develop (41) in the same way as above, obtaining:

$$\begin{aligned} U^{n+1} - U^n + & f\big[\big(u^n - (u^* - u^\dagger)\big)\Delta t + \sigma\Delta B_t\big](U^n) \\ & -\frac{1}{2}f\big[\big(u^n - (u^* - u^\dagger)\big)\Delta t + \sigma\Delta B_t\big]\Big(f\big[\big(u^n - (u^* - u^\dagger)\big)\Delta t + \sigma\Delta B_t\big](U^n)\Big) = 0, \end{aligned}$$

which by virtue of Propositions 4 is consistent with (20). □

Remark 7 (Convergence order)**.** *It is important to note that, theoretically, these schemes still have a (probabilistic) strong convergence order of* $1/2$ *(i.e., the same order as Euler-Maruyama) . Although, parallels are drawn with the Milstein scheme in C, which is of strong order one, this convergence order does not hold when the Lévy area is removed, as considered in LU schemes to improve accuracy (Boulvard and Mémin, 2024; Fiorini et al., 2023). However, numerically, the observed convergence order,* γ*, lies within* $1/2 < \gamma < 1$*, and a significantly reduced error constant (Fiorini et al., 2023), making these schemes particularly appealing.*

Those schemes are further studied for the LU Saint-Venant equationsin the next section.

4 Discretization

Our goal is to show here how a positivity-preserving LU Saint-Venant scheme may be derived as a variation of a deterministic finite-volume scheme implemented in (Rigal, 2022). To draw a bridge between the properties of the discretizations of classical and LU Saint Venant respectively, we will use the example of the 1D Rusanov discretizations which we describe below.

4.1 1-D Riemann invariants

The first step in studying the discretizations is to compute the Rieman invariant, which characterize the wave-like behaviour of solutions. Going back to the original presentation of the Saint-Venant equations, both the LU and classical versions (11), (13) may be expressed under the compact generic form:

$$\partial_t h + \big(\alpha^{\mathrm{d}t,\mathrm{d}B_t}\partial_x\big)h + h(\partial_x u)\mathrm{d}t = 0, \tag{42a}$$

$$\partial_t u + \big(\alpha^{\mathrm{d}t,\mathrm{d}B_t}\partial_x\big)u + g\partial_x h\mathrm{d}t = 0. \tag{42b}$$

We now seek the Riemann invariants of this dynamic. Multiplying the first equation by $\sqrt{\frac{g}{h}}$, we rewrite (42) in the following way:

$$\begin{aligned}\partial_t(2\sqrt{gh}) + \big(\alpha^{\mathrm{d}t,\mathrm{d}B_t}\partial_x\big)(2\sqrt{gh}) + \sqrt{gh}(\partial_x u)\mathrm{d}t = 0,\\ \partial_t u + \big(\alpha^{\mathrm{d}t,\mathrm{d}B_t}\partial_x\big)u + \sqrt{gh}\,\partial_x 2\sqrt{gh}\mathrm{d}t = 0;\end{aligned}$$

By subtracting the first equation from the second, first, and then by adding the two equations, we obtain respectively:

$$\begin{aligned}\partial_t(u - 2\sqrt{gh}) + \big((\alpha^{\mathrm{d}t,\mathrm{d}B_t} - \sqrt{gh}\mathrm{d}t)\partial_x\big)(u - 2\sqrt{gh}) = 0,\\ \partial_t(u + 2\sqrt{gh}) + \big((\alpha^{\mathrm{d}t,\mathrm{d}B_t} + \sqrt{gh}\mathrm{d}t)\partial_x\big)(u + 2\sqrt{gh}) = 0.\end{aligned}$$

Under this formulation, we obtain the following Riemann invariants:

$$R_- = u - 2\sqrt{gh}, \quad R_+ = u + 2\sqrt{gh}, \tag{43}$$

and associated advections:

$$\lambda_-[\alpha^{\mathrm{d}t,\mathrm{d}B_t}] = \alpha^{\mathrm{d}t,\mathrm{d}B_t} - \sqrt{gh}\mathrm{d}t, \quad \lambda_+[\alpha^{\mathrm{d}t,\mathrm{d}B_t}] = \alpha^{\mathrm{d}t,\mathrm{d}B_t} + \sqrt{gh}\mathrm{d}t. \tag{44}$$

Therefore modifying the advection does not modify the Riemann invariants, that is the characteristic lines associated with the system but it does alter the velocity of propagation of these characteristics. Let us now bring the comparison between the Rusanov's scheme under both the classical and LU formulations of the Saint-Venant equations.

4.2 Rusanov's scheme

We consider a regular Cartesian mesh for our domain:

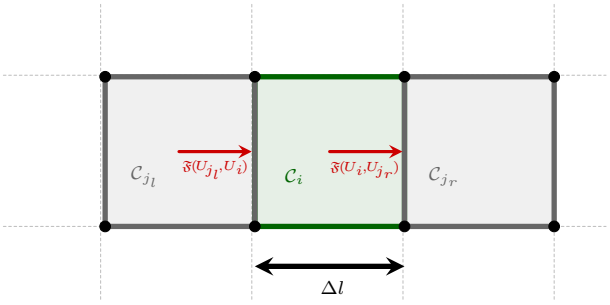

Figure 2: Mesh over domain, $U_i := U(\mathcal{C}_i)$ and $\alpha_i^{\Delta t,\Delta B_t} := \alpha^{\Delta t,\Delta B_t}(\mathcal{C}_i)$

We now define the Rusannov flow from a left cell to a right cell:

$$\mathfrak{F}[\alpha^{\Delta t,\Delta B_t}](U_{\text{left}},U_{\text{right}}) := \frac{F[\alpha_{\text{right}}^{\Delta t,\Delta B_t}](U_{\text{right}}) + F[\alpha_{\text{left}}^{\Delta t,\Delta B_t}](U_{\text{left}})}{2} - \Lambda_{\text{left,right}}^{\Delta t,\Delta B_t}\frac{U_{\text{right}} - U_{\text{left}}}{2}, \tag{45}$$

where

$$\Lambda_{\text{left,right}}[\alpha^{\Delta t,\Delta B_t}] := \max_{\cdot=-,+} \max_{*=\text{left,right}} \{|\lambda_\cdot[\alpha_*^{\Delta t,\Delta B_t}](U_*)|\}. \tag{46}$$

Now considering our cell $\mathcal{C}_i$ and summing all contributions we set the following scheme:

$$U_i^* - U_i + \frac{\Delta t}{\Delta l}\big(\mathfrak{F}[\alpha^{\Delta t,\Delta B_t}](U_i, U_{j_r}) - \mathfrak{F}[\alpha^{\Delta t,\Delta B_t}](U_{j_l}, U_i)\big) = 0. \tag{47}$$

First let us recall a property of the classical Rusanov flux

Lemma 7 (Positivity of water height for deterministic Rusanov flux)**.** *Under CFL condition:*

$$\big(1 - \frac{\Delta t}{2\Delta l}(\Lambda_{i,j_r}[u\Delta t] + \Lambda_{i,j_l}[u\Delta t])\big) \geq 0,$$

the scheme

$$U_i^* - U_i + \frac{\Delta t}{\Delta l}\big(\mathfrak{F}[u\Delta t](U_i, U_{j_r}) - \mathfrak{F}[u\Delta t](U_{j_l}, U_i)\big) = 0. \tag{48}$$

preserves the positivity of the water height i.e:

$$h_i \geq 0, \quad \forall i \implies h_i^* \geq 0, \quad \forall i$$

This naturally extends to our generalized Rusanov flux:

Lemma 8 (Positivity of water height of generalized Rusanov flux)**.** *Under CFL condition:*

$$\Big(1 - \frac{\Delta t}{2\Delta l}\big(\Lambda_{i,j_r}[\alpha^{\Delta t,\Delta B_t}] + \Lambda_{i,j_l}[\alpha^{\Delta t,\Delta B_t}]\big)\Big) \geq 0$$

the scheme (47) *preserves the positivity of the water height i.e:*

$$h_i \geq 0, \quad \forall i \implies h_i^* \geq 0, \quad \forall i$$

Proof. We start by including the expressions of the flow in formulation (47), which yields:

$$U_i^* - U_i + \frac{\Delta t}{\Delta l}\Big[\big(\frac{F[\alpha^{\Delta t,\Delta B_t}](U_{j_r}) - F[\alpha^{\Delta t,\Delta B_t}](U_{j_l})}{2}\big) - \Lambda_{i,j_r}^{\Delta t,\Delta B_t}\frac{U_{j_r} - U_i}{2} + \Lambda_{i,j_l}^{\Delta t,\Delta B_t}\frac{U_i - U_{j_l}}{2}\Big] = 0.$$

We then reshuffle this expression into:

$$\begin{aligned} U_i^* = U_i\big(1 - \frac{\Delta t}{2\Delta l}(\Lambda_{i,j_r} + \Lambda_{i,j_l})\big) &+ \frac{\Lambda_{i,j_r}^{\Delta t,\Delta B_t}\Delta t}{2\Delta l}\big(U_{j_r} - \frac{1}{\Lambda_{i,j_r}^{\Delta t,\Delta B_t}}F[\alpha^{\Delta t,\Delta B_t}](U_{j_r})\big) \\ &+ \frac{\Lambda_{i,j_l}^{\Delta t,\Delta B_t}\Delta t}{2\Delta l}\big(U_{j_l} + \frac{1}{\Lambda_{i,j_l}^{\Delta t,\Delta B_t}}F[\alpha^{\Delta t,\Delta B_t}](U_{j_l})\big). \end{aligned}$$

Applying this to the water height, we get:

$$h_i^* = h_i\big(1-\frac{\Delta t}{2\Delta l}(\Lambda_{i,j_r}+\Lambda_{i,j_l}+\Lambda_{i,j_t}+\Lambda_{i,j_b})\big)+\frac{\Lambda_{i,j_r}^{\Delta t,\Delta B_t}\Delta t}{2\Delta l}\big(h_{j_r}-\frac{1}{\Lambda_{i,j_r}^{\Delta t,\Delta B_t}}\alpha_x^{\Delta t,\Delta B_t}h_{j_r}\big) + \frac{\Lambda_{i,j_l}^{\Delta t,\Delta B_t}\Delta t}{2\Delta l}\big(h_{j_l}+\frac{1}{\Lambda_{i,j_l}^{\Delta t,\Delta B_t}}\alpha_x^{\Delta t,\Delta B_t}h_{j_l}\big).$$

Now, let us notice that

$$|\alpha_x^{\Delta t,\Delta B_t}| \leq \max_{\cdot=-,+}\{|\lambda_\cdot^{\Delta t,\Delta B_t}(U_i)|\} \leq \Lambda_{i,j_r}^{\Delta t,\Delta B_t},$$

hence

$$\big(h_{j_r}-\frac{1}{\Lambda_{i,j_r}^{\Delta t,\Delta B_t}}\alpha_x^{\Delta t,\Delta B_t}h_{j_r}\big)\geq 0.$$

The same goes for the other components, therefore:

$$h_i^* \geq h_i\big(1-\frac{\Delta t}{2\Delta l}(\Lambda_{i,j_r}+\Lambda_{i,j_l})\big),$$

which yields the positivity of the water height under the CFL. □

We can now apply this result to state that all three of our schemes, (39), (40) and (41), preserve the positivity of the water's height under suitable CFL conditions.

Remark 8. *The specific choices of the advection in schemes* (39),(40) *and* (41) *guarantee that the CFL condition can be defined a priori to the computations, thus ensuring that our scheme are defined on a finitely small time step.*

5 Algorithm description

5.1 General algorithm

We shall now delve deeper into the generation of this generalized advection, focusing specifically on its main difficulty: noise parametrization. Various modeling choices can be made for this purpose. Examples of data-driven strategies and pure model-based schemes are provided and assessed for quasi-geostrophic models and shallow water models in (Bauer et al., 2020b; Brecht et al., 2021; Li et al., 2023; Resseguier et al., 2021). In this work, we will particularly explore a noise term defined from the resolved velocity variables through a self-similarity assumption. This model has the advantage of not requiring high-resolution data.

5.2 Parametrization of the noise

Heuristically, we consider the noise as the factor that causes the velocity fields to fluctuate around a statistical average. The noise parameterization involves two main steps: first, recovering or providing an ansatz for these fluctuations, and second, deriving their covariation, which is then used as the primary scaling parameter for the noise.

Recovering the fluctuations: As explained above, the fluctuations are considered around a statistical average, and the choice of methods largely depends on how we define this average. We have three main options:

- *true statistical average*: This involves running several parallel simulations of the system with small initial perturbations and observing the resulting fluctuations.
- *time average*: Based on an ergodicity argument, we examine the fluctuations of the speed within each cell $\mathcal{C}_i$ around its time average, which we refer to as pseudo-observations.
- *space average*: Here, the pseudo-observations are derived from the spatial heterogeneity (i.e. with respect to a space average) of our variables.

In this study, we focus on the latter case: fluctuation pseudo-observations with respect to a space average. The computation process can be described as follows. Around each cell, $\mathcal{C}_i$, of the simulation mesh, we construct a frame of neighboring cells. From this frame, we first derive a local average of the velocity fields. The pseudo-observation, u_{po}, is then defined as the difference between this local average, $\bar{u}$, (at the cell center) and the velocity at a neighboring point selected at random.

A cell-wise pseudo observation $\tilde{u}_i$ is hence defined as a random fluctuation from the local spatial average i.e

$$\tilde{u}_i = u_{po,i} - \bar{u}_i.$$

These fluctuations are then computed simultaneously for all cells to build a pseudo observation field $\tilde{u} := (\tilde{u}_i)_i$; reiterating this procedure p times we build a set of several pseudo-observation fields $(\tilde{u}^1, \dots, \tilde{u}^p)$:

$$\tilde{u} := \left(\tilde{u}^1, \dots, \tilde{u}^p\right) := \begin{pmatrix} \tilde{u}_1^1 & \dots & \tilde{u}_1^p \\ \vdots & \vdots & \vdots \\ \tilde{u}_m^1 & \dots & \tilde{u}_m^p \end{pmatrix},$$

where m stands for the number of cells of the grid, while p is the number of pseudo observations (i.e. random draws at each cell). This noise model amounts to consider a self-similarity assumption of the small scales. The spatial distribution of the unresolved variables is directly set from the random fluctuations

of the resolved velocity. Let us note that, with this definition, the noise is intrinsically small for smooth fields and within sufficiently small neighbourhoods. This reflects the idea that the stochastic model should converge to the deterministic model, with the noise amplitude gradually decreasing as the resolution approaches a high-resolution reference.

Noise model: The pseudo-observations random draws $\{\tilde{u}^{(j)}, j = 1, \ldots, p\}$ are considered to be observations of a m dimensionnal Wiener process with correlation operator σ:

$$\tilde{u}^{(j)} = \left(\sigma \mathrm{d}B_t\right)^{\omega_j} \tag{49}$$

Because of its Gaussian properties this stochastic process admits a Kahrunen-Loève expansion:

$$\sigma \mathrm{d}B_t = \sum_{i=1}^{p-1} \sqrt{\lambda_i}\phi_i \mathrm{d}B_t^i,$$

where the $(\phi_i)_{i=1\ldots p-1}$ and the $(\lambda_i)_{i=1\ldots p-1}$ are the eigenvectors and corresponding eigenvalues of the symetrized covariance matrix $\sigma^T\sigma$ obtained by spectral decomposition; this technique is alternatively called proper orthogonal decomposition (POD) or singular value decomposition (SVD).

This spectral representation conveniently provides the symmetric covariation, as $\sigma^T\sigma \simeq \sum \lambda_i \phi_i \phi_i^T$. Once the structure of the noise (5.2) is obtained the coefficients $\mathrm{d}B_t^i$ are simulated as Gaussian random variables and thus the stochastic part of the advection $\alpha^{n,\Delta t,\Delta B_t}$ is derived. Its additional deterministic components are also computed from σ.

6 Results

The following two sections provide a numerical assessment of our methods along two complementary directions. The first examines the effects of different parameterizations of our model in an idealized doubly periodic test case illustrating the development of waves. The second focuses on validating our results against observational data in a realistic scenario replicating the conditions of the 1993 Hokkaido-Nansei-Oki tsunami in Monai Valley.

7 Simplified testcase

To validate the essential features of our model we have first used a sandbox testcase in which a water column is initially released from a corner of the domain with periodic boundary conditions (cf figure 3 showing typical water height evolution for the deterministic and stochastic evolutions).

As can be immediately observed from this example, the stochastic setting exhibits rougher solutions with the emergence of small-scale waves that do not arise in the deterministic case. As exemplified in the following, this sand-box example allowed us to confirm that the stochastic solutions remain stable in

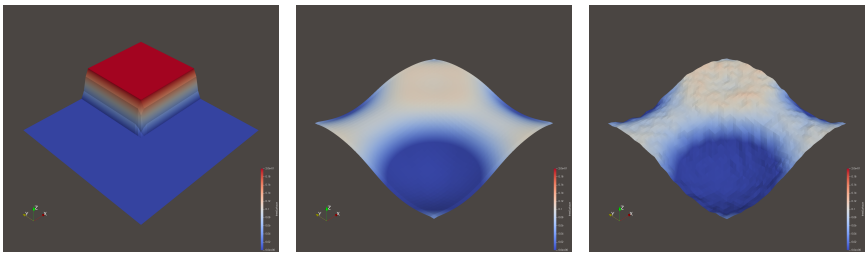

Figure 3: Water release testcase, from left to right, up to bottom: (a) Initial state of the simulation; (b) Intermediary state of the deterministic simulation;(c) Intermediary state of the simulation with advection noise

time for various resolution and hence for different magnitude of the noise. This stability can be attributed to the strong balance between the energy introduced by the noise and the dissipation inherently associated with it. This benchmark also enables an initial, straightforward analysis of the features of our schemes by comparison with a high-resolution deterministic model used as a reference.

First, in figure 4 we analyse the differences between a high-resolution deterministic model of resolution 160×160 (serving as a ground-truth reference) and our deterministic and stochastic models both with the delayed advection (40) and with the predicted advection (41). We observe that for small-scale noise,

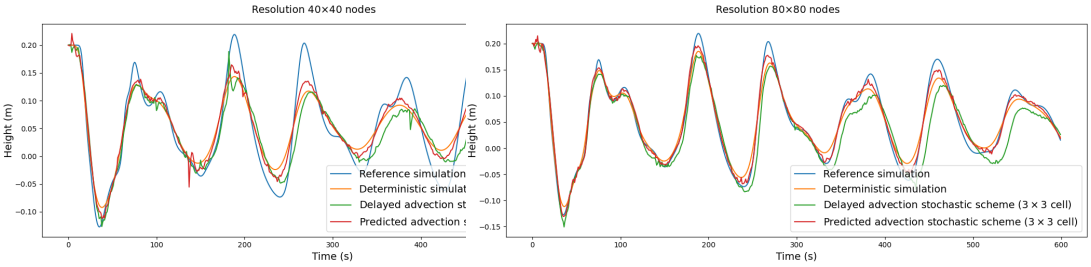

Figure 4: Comparison of deterministic and stochastic time series – height (in cm) againt time (in s) – in the water release experiment.The evolution of the wave in the deterministic and stochastic settings are compared at different resolution, left: resolution of 40×40, right: resolution of 80×80 ; The transport noise considered is assumed to correspond to the smallest spatial scales of the simulation as it generated on fluctuations computed over a 3×3 neighborhood.

both stochastic schemes exhibit slight temporal shifts in the results, which in turn lead to higher errors: at low resolution for the predicted advection schemes, and at high resolutions for the delayed advection scheme. Overall, the predicted advection schemes better preserve the simulation dynamics. These errors are illustrated by bar diagrams in Figure 7. Especially at finer resolutions, the delayed advection scheme produces noticeably higher errors compared to the predicted advection scheme. The deterministic scheme yields the best results at

higher resolutions, particularly in the presence of small-scale noise.

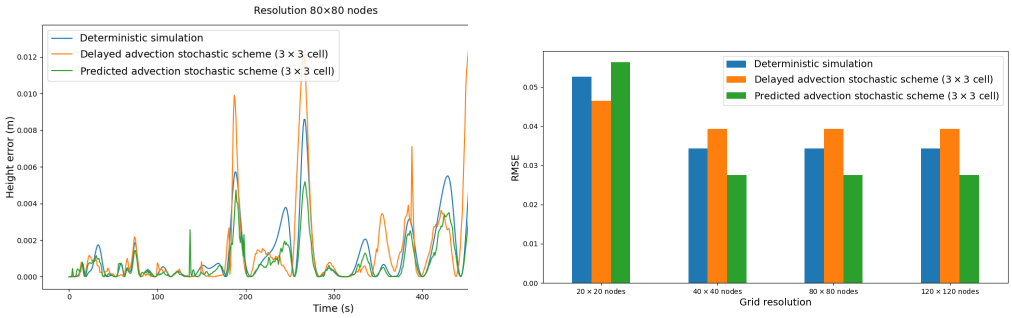

Figure 5: Error time series resolution of 80×80 (left) – height (in cm) against time (in s) and cumulated error – RMSE against resolution – with respect to high-resolution simulation.

Next, focusing on the stochastic model with predicted advection (41), we test the impact on the simulation of the neighborhood size in the noise definition (cf figure 6).

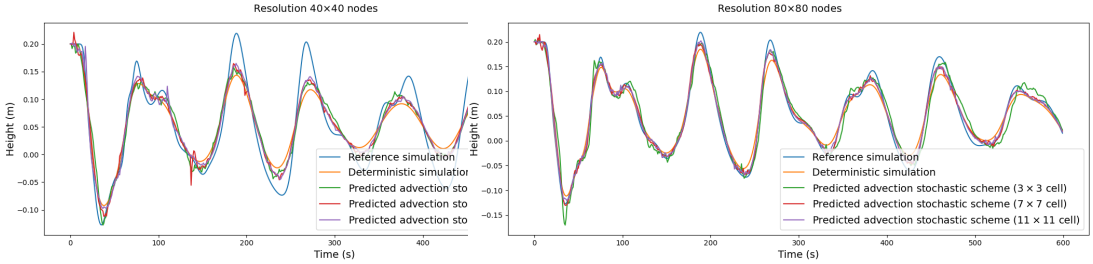

Figure 6: Comparison of different noise definitions for stochastic scheme in the water release experiment, time series – height (in cm) against time (in s) – , left: resolution of 40×40, right: resolution of 80×80.

It now appears that defining noise over a wider neighborhood (i.e., with larger spatial scales) consistently reduces the scheme's error and further enhances the dynamics. Clearly, the noise scale impacts the results. Given that the noise considered here is based on a self-similarity assumption for solution fluctuations, it is likely that this assumption aligns better with large-scale noise than with noise at scales close to the simulation's resolution cutoff. At very coarse resolution, both deterministic and stochastic solutions show results with low wave amplitude and exhibit significant errors. The stochastic simulation also shows a phase shift relative to the deterministic setting. As highlighted in previous studies (Brecht et al., 2021; Tucciarone et al., 2025), at coarse resolution only data-driven noise significantly improves the results of the corresponding deterministic model. Notably, at this resolution, only the delayed advection

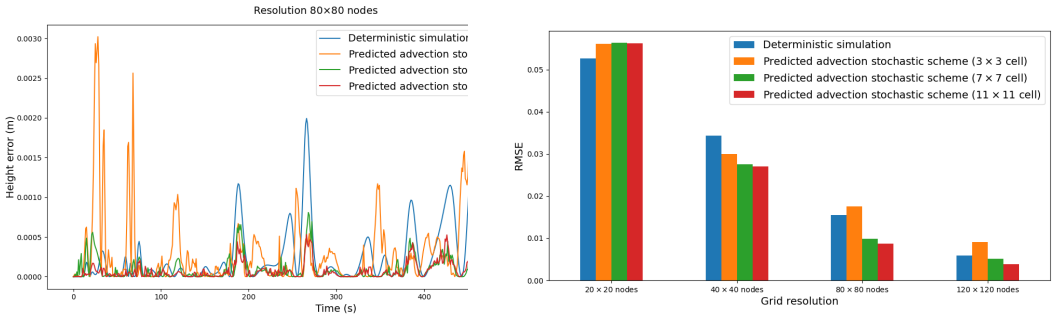

Figure 7: Error time series (left) – height (in cm) against time (in s) –and cumulated error (right) – RMSE against resolution – with respect to high-resolution simulation comparizon of different spatial scale for the noise; Except for the lowest resolution (for which the delayed advection scheme performs better), enlarging the noise spatial scale leads to a lowering of the error.

scheme does not exhibit phase shifting (see Fig. 7). Therefore, delayed advection appears preferable for very low resolutions. However, since our focus here is more on higher resolutions and the influence of noise scale, we chose to assess only the predicted advection scheme, which has demonstrated strong performance at higher resolutions in terms of wave amplitude. For resolutions ranging from 40×40 to 120×120, the stochastic solutions with expanded noise scales outperform the deterministic case.

We now complete the study of this testcase with an ensemble of $N = 40$ simulations to better understand the uncertainty propagation properties of our scheme. Simulating an ensemble of realizations allows us to highlight several

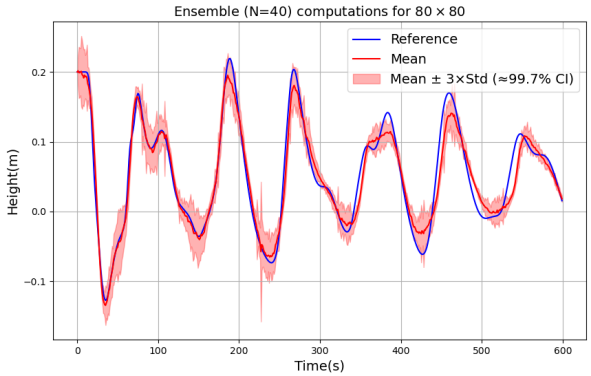

Figure 8: Time-series for the ensemble $N = 40$ computations. Height (in cm) against time (in s) with resolution of 80×800.

features of the stochastic model. In particular, the variance of the realizations concentrates in time near the inflection points of the free-surface elevation, enabling the ensemble to better match the reference solution at the extrema.

To further evaluate the proposed models, we will now focus our study on a realistic experimental benchmark.

8 Monai valley benchmark

The Monai Valley benchmark is an initiative by the NOAA Center for Tsunami Research, designed to assess the reliability of numerical tsunami simulation models. The primary goal of this benchmark is to provide a set of reference data that can test the validity of numerical models by accurately reproducing the behavior of tsunamis when they encounter complex coastal environments. To achieve this, the benchmark relies on a scaled-down physical model (1/400) of the Monai Valley, replicating the conditions of the 1993 Hokkaido-Nansei-Oki tsunami. This model allows researchers to observe the dynamic interactions between the tsunami and coastal topography, thus offering valuable insights for improving predictive models. The data obtained from this benchmark are then used to compare the results of numerical simulations with real-world experimental measurements, which is crucial for refining the accuracy of the models and strengthening confidence in their ability to predict potential flood zones during future tsunami events.

We now compare both the delayed advection scheme (40) and the predicted advection sheme (41), along with their their deterministic counterpart, within the Monai valley benchmark. The experimental data were collected at three separate measurement locations, referred to as "channels" (numbered 5-7-9). For each channel, we compared our simulations at different spatial resolutions, as well as the squared errors and RMSE associated with those schemes. We present our results for channel 9 in figures 9 and 10. For all the stochastic simulations we used a neighborhood of (7×7), to define the noise scale, as this provided favorable results in the previous benchmark. As was done for the sandbox

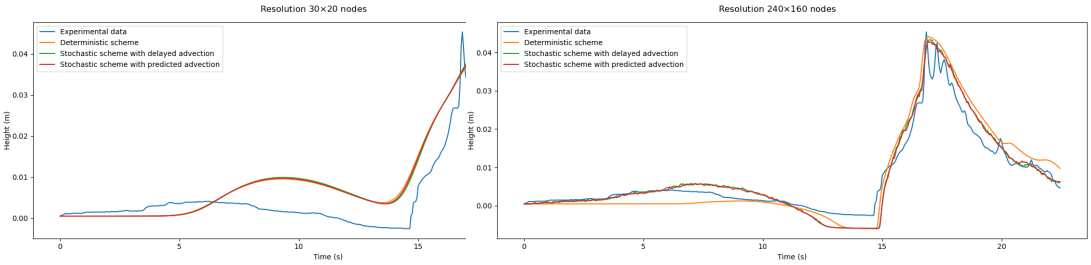

Figure 9: Free surface time-series height (in cm) against time (in s) at channel 9, left: resolution of 30×20, right: resolution of 240×160.

testcase, we conclude this experiment with the simulation of an ensemble of

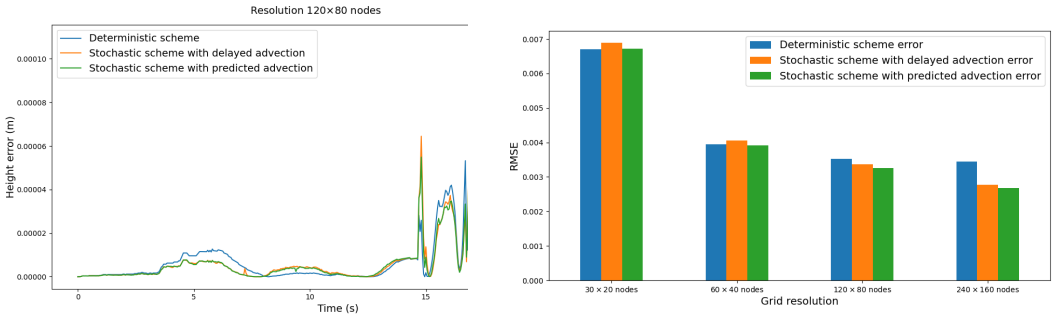

Figure 10: Error time series (left) – height (in cm) against time (in s) – and Cumulated error (right) – RMSE against resolution – for experimental data at channel 9.

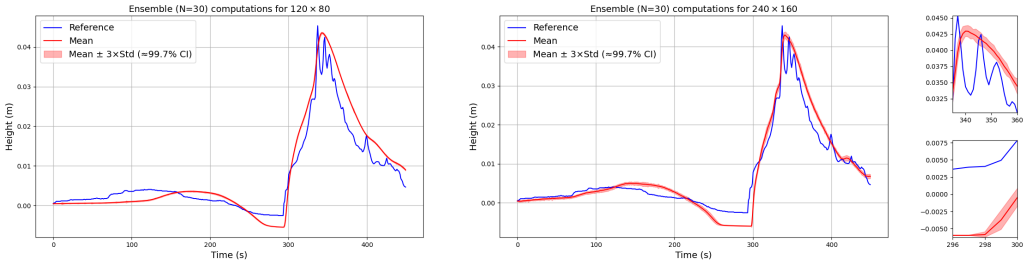

Figure 11: Time-series for the ensemble $N = 30$ computations Height (in cm) against time (in s) at channel 9, left: resolution of 120×800, right: resolution of 240×160.

realizations. results are broadly consistent with those obtained for the idealized testcase, with the largest noise deviations occurring near the inflection points. However, the influence of our stochastic scheme under the chosen self-similar noise parametrization appears less pronounced than in the idealized setting. It is also noteworthy that higher resolutions lead to better results as illustrated in Fig. 10, which confirms the increased benefit of these stochastic models at higher resolution as already observed in the idealistic benchmark. It can also be noted that, despite the relatively weak amplitude of the noise (as evidenced by the small ensemble variance), the stochastic simulation departs from the deterministic one and provides a better fit to the data.

Overall, the stochastic delayed advection scheme (40) and the stochastic predicted advection scheme (41) both lead to a reduction of the cumulative error, while maintaining a comparable ease of implementation and requiring no data-driven noise input. The effect of these stochastic schemes is particularly striking

in the high-resolution case – an unexpected outcome, given that the LU model was originally conceived as a subgrid parametrization to compensate for the lack of fine-scale dynamics in coarse-grid models. This result nonetheless suggests that high-resolution deterministic models may not represent the pinnacle of CFD accuracy; the introduction of noise, as done within the LU framework, may further refine the model dynamics. In particular, it may counteract the numerical diffusion inherent to the discretization (as illustrated in the sandbox testcase). A more thorough analysis of the interplay between numerical diffusion and the excitation induced by LU noise would be a valuable extension of this work.

It is also noteworthy that the added value of the stochastic models is less pronounced in the realistic testcase than in the sandbox scenario. This likely stems from the fact that the Shallow Water model – being the simplest in the hierarchy of nonlinear wave models – does not accurately reproduce the experimental measurements from Monai Valley, whereas it serves as an exact reference model in the sandbox setup. Stochastic versions of the Serre-Green-Naghdi or Boussinesq wave models, as proposed in (Debussche et al., 2024a), could potentially yield improved agreement with the experimental data. Moreover, data-driven noise or waveform perturbations, as suggested in (Debussche et al., 2024a; Mémin et al., 2024), could be considered to enhance the noise parametrization. These directions, however, lie beyond the scope of the present study and are left for future work.

9 Conclusion and discussion

This study has enhanced our understanding of second-order numerical schemes proposed in the context of models built from stochastic transport principles (Boulvard and Mémin, 2024; Fiorini et al., 2023; Li et al., 2023). The development of several discrete schemes has been justified based either on the discretized Itô-Wentzell formula or as particular cases of Milstein schemes, where the Lévy area is neglected. These schemes have been further discussed in the context of the Shallow Water model. Numerical assessments have demonstrated the good performance of the method with noise based on a self-similarity assumption of small-scale fluctuations. This model-based noise, which relies solely on the current simulation, allows us to achieve better results than the corresponding deterministic scheme at higher resolutions. For coarse resolutions, data-driven noise should be utilized to enhance the deterministic solution (Bauer et al., 2020b; Brecht et al., 2021; Li et al., 2023).

Acknowledgments

The authors would like to thank Mathieu Rigal for his help with the numerical simulations. The authors also acknowledge the support of the ERC EU project 856408-STUOD and the Inria challenge SURF (Sea Uncertainty Representation

and Forecast).

A Quadratic (co-)variation

In stochastic calculus, quadratic covariation (or cross-variance) of two processes X and Y play a fundamental role. Quadratic variation is a bounded variation process is defined as:

$$\big\langle X, Y \big\rangle_t = \lim_{n \to 0} \sum_{i=1}^{p_n} (X_i^n - X_{i-1}^n)(Y_i^n - Y_{i-1}^n), \tag{50}$$

where $0 = t_0^n < t_1^n < \cdots < t_{p_n}^n = t$ is a partition of the interval $[0, t]$ and this limit, if it exists, is defined in the sense of convergence in probability.

Assuming that X and Y are two continuous semimartingales, defined as $X_t = X_0 + A_t + M_t, Y_t = Y_0 + B_t + N_t$ with M, N martingales and A, B finite variation processes, then their quadratic covariation (50) exists, and is given by

$$\big\langle X, Y \big\rangle_t = \big\langle M, N \big\rangle_t. \tag{51}$$

In particular, the quadratic variation of a standard Brownian motion B (as a martingale) is given by $\langle B \rangle_t = t$, the quadratic variation of two bounded variation processes f, and g (such as deterministic functions) can be shown to be zero ($\langle f, g \rangle_t = 0$), as well as the covariation between a martingale and a bounded variation process ($\langle f, M \rangle_t = 0$).

The quadratic (co-)variations play an important role in the Itô calculus and its generalization of the chain rule. In particular, they are involved in the Itô integration by parts formula:

$$\mathrm{d}(X_t Y_t) = X_t \mathrm{d}Y_t + Y_t \mathrm{d}X_t + \mathrm{d}\langle X, Y \rangle_t. \tag{52}$$

The quadratic variation of the Itô integrals of two adapted processes with respect to martingale, M and N, respectively, is provided by the following important formula:

$$\Big\langle \int_0^{\cdot} \Theta_s \mathrm{d}M_s, \int_0^{\cdot} \Theta'_s \mathrm{d}N_s \Big\rangle_t = \int_0^t \Theta_s \Theta'_s \mathrm{d}\big\langle M, N \big\rangle_t \tag{53}$$

This property is involved in the Itô isometry, allowing to express the covariance of two Itô integrals:

$$\mathbb{E}\Big[\big(\int_0^t f \mathrm{d}M_s \big) \big(\int_0^t g \mathrm{d}N_s \big) \Big] = \mathbb{E}\Big[\int_0^t fg \, \mathrm{d}\big\langle M, N \big\rangle_s \Big], \tag{54}$$

where f and g are two adapted processes such that $\int_0^t f^2 \mathrm{d}\big\langle M, M \big\rangle_s$ and $\int_0^t g^2 \mathrm{d}\big\langle N, N \big\rangle_s$ are integrable.

B Conversions between Itô and Stratonovich integrals

The following theorem provides a general Stratonovich–Itô–integral conversion rule (Kunita, 1990):

Theorem 1. *If X and Y are two continuous semimartingales, the following Stratonovich integral is well defined:*

$$X_t \circ \mathrm{d}Y_t = X_t \mathrm{d}Y_t + \frac{1}{2}\mathrm{d}\big\langle X, Y \big\rangle_t. \tag{55}$$

This theorem is very useful to move from Itô to Stratonovich integral. In (Bauer et al., 2020a) it is used to express the transport operator in Stratonovich representation. The pro and cons of both integrals for geophysical modelling are also analyzed.

C Interpretations of double advection

While we have provided in section 3 a proof of consistency for the schemes of subsection 3.5, we seek here to gain a better insight at the essential causes of this result. To do so, we shall here offer two interpretations of the role played by the second order in stochastic integration. In the first interpretation we explore the discretization of the Itô integral and of Itô calculus in order to reformulate the Itô-Wentzell (total variation) formula (TVF) and thus, the stochastic material derivative (6) which is at the roots of the LU models and of the integration schemes of section 3. The second approach is centered on second-order, Milstein schemes, applied to the stochastic integral. Surprisingly both approaches allow us to converge toward broadly the same interpretation, something that we will try to explain in conclusion of this part.

C.1 Discretized interpretation of the total variation formula

The objective addressed in this appendix is aims to further explore the proofs from Section 3, in examining the fundamental components of the stochastic material derivative. Specifically, we reformulate the Itô-Wentzell formula to allow us to rewrite (**quadratic term**) as a double advection. We then reformulate (**cross term**) within the framework of the LU formalism, also as a double advection.

C.1.1 Expansion of a stochastic functionnal and Itô-Wentzell formula

We recall first that our framework consists of the regularity requirements of definitions 3 and 4. We start from a simple decomposition of the variation of a

stochastic functionnal of a stochastic variable:

$$\theta_T(X_T) = \theta_0(X_0) + \sum_{k=0}^{n-1} \theta_{t_{k+1}}(X_{t_k}) - \theta_{t_k}(X_{t_k}) + \sum_{k=0}^{n-1} \theta_{t_{k+1}}(X_{t_{k+1}}) - \theta_{t_{k+1}}(X_{t_k}).$$

Here, we identify a time variation quantity in the first term on the right-hand side, which we will not examine further, and a second term that is more intricate. We have the following Taylor expansion of the latter:

Lemma 9. *The following integral remainder Taylor expansion:*

$$\begin{aligned}
&\sum_{k=0}^{n-1} \theta_{t_{k+1}}(X_{t_{k+1}}) - \theta_{t_{k+1}}\ (X_{t_k}) \\
&= \sum_{k=0}^{n-1} \frac{\partial}{\partial x}\theta_{t_{k+1}}(X_{t_k}) \cdot \Delta X_{t_k} + \big(\int_0^1 \frac{\partial^2}{\partial x^2}\theta_{t_{k+1}}(X_{t_k} + \alpha\Delta X_{t_k})(1-\alpha)\mathrm{d}\alpha\big) : \Delta X_{t_k} \otimes \Delta X_{t_k} \\
&= \sum_{k=0}^{n-1} \frac{\partial}{\partial x}\theta_{t_k}(X_{t_k}) \cdot \Delta X_{t_k} \quad + \sum_{k=0}^{n-1} \big(\frac{\partial}{\partial x}\theta_{t_{k+1}}(X_{t_k}) - \frac{\partial}{\partial x}\theta_{t_k}(X_{t_k})\big) \cdot \Delta X_{t_k} \\
&\qquad\qquad + \sum_{k=0}^{n-1} \big(\int_0^1 \frac{\partial^2}{\partial x^2}\theta_{t_{k+1}}(X_{t_k} + \alpha\Delta X_{t_k})(1-\alpha)\mathrm{d}\alpha\big) : \Delta X_{t_k} \otimes \Delta X_{t_k}
\end{aligned} \tag{56}$$

yields the Taylor-Lagrange expansion:

$$\begin{aligned}
&\sum_{k=0}^{n-1} \theta_{t_{k+1}}(X_{t_{k+1}}) - \theta_{t_{k+1}}(X_{t_k}) \\
&= \sum_{k=0}^{n-1} \frac{\partial}{\partial x}\theta_{t_k}(X_{t_k}) \cdot \Delta X_{t_k} \quad + \sum_{k=0}^{n-1} \big(\frac{\partial}{\partial x}\theta_{t_{k+1}}(X_{t_k}) - \frac{\partial}{\partial x}\theta_{t_k}(X_{t_k})\big) \cdot \Delta X_{t_k} \\
&\qquad\qquad + \sum_{k=0}^{n-1} \frac{1}{2}\frac{\partial^2}{\partial x^2}\theta_{t_{k+1}}(\xi_{t_k}) : \Delta X_{t_k} \otimes \Delta X_{t_k} \ \textit{ with } \xi_{t_k} = \frac{1}{2}(X_{t_{k+1}} + X_{t_k})
\end{aligned} \tag{57}$$

Proof. The gap between both formulas is bridged by the application of the mean-value theorem to the last right-hand term. □

We have contrasted the Taylor expansion with the integral remainder formula against the Taylor-Lagrange formula. While the former serves as the foundation of our construction, the latter is the more classical approach used in proving the Itô-Wentzell (total variation) formula, as outlined, for example, in (Kunita, 1990).

Proposition 5. *Itô-Wentzell formula. We have the following convergences (in probability) of the components of the expansion of θ:*

$$\sum_{k=0}^{n-1} \theta_{t_{k+1}}(X_{t_k}) - \theta_{t_k}(X_{t_k}) \xrightarrow{n\to\infty} \int_0^T \mathrm{d}_s\theta_s(X_t)$$

$$\sum_{k=0}^{n-1} \frac{\partial}{\partial x}\theta_{t_k}(X_{t_k}) \cdot \Delta X_{t_k} \xrightarrow{n\to\infty} \int_0^T (\mathrm{d}X_t \cdot \nabla)\theta_t(X_t),$$

$$\sum_{k=0}^{n-1} \big(\frac{\partial}{\partial x}\theta_{t_{k+1}}(X_{t_k}) - \frac{\partial}{\partial x}\theta_{t_k}(X_{t_k})\big) \cdot \Delta X_{t_k} \xrightarrow{n\to\infty} \int_0^T \sum_{i=1}^d \mathrm{d}\langle \frac{\partial}{\partial x_i}\theta_\cdot(X_\cdot), X^i_\cdot\rangle_t,$$

$$\sum_{k=0}^{n-1} \frac{1}{2}\frac{\partial^2}{\partial x^2}\theta_{t_{k+1}}(\xi_{t_k}) : \Delta X_{t_k} \otimes \Delta X_{t_k} \xrightarrow{n\to\infty} \int_0^T \frac{1}{2}\frac{\partial^2}{\partial x^2}\theta_t(X_t) : \mathrm{d}\langle X\rangle_t.$$

hence:

$$(57) \xrightarrow{n\to\infty} (\mathrm{TVF}),$$
$$\textit{Right-hand term of } (57) \xrightarrow{n\to\infty} \mathbb{D}_t.$$

Thanks to Lemma 9 this last result admits the following corollary:

Corollary 5. *The integral remainder Taylor expansion* (56) *yields the Itô-Wentzell (total variation) formula:*

$$(56) \xrightarrow{n\to\infty} (\mathrm{TVF}),$$
$$\textit{Right-hand term of } (56) \xrightarrow{n\to\infty} \mathbb{D}_t$$

Proof. Here we only need to remark that both the left-hand and right-hand parts of (56) and (57) are the same and therefore, converge to the same limits □

In the next part we will work to reformulate the components of (56) to give rise to a new expansion of our stochastic process in which the discretizations of the (**quadratic term**) and the (**cross term**) are replaced by that of the (**double advection**).

Proposition 6. *The integral remainder Taylor expansion* (56) *admits the following reformulation:*

$$\begin{aligned}
&\sum_{k=0}^{n-1} \theta_{t_{k+1}}(X_{t_{k+1}}) - \theta_{t_{k+1}}(X_{t_k}) \\
=&\sum_{k=0}^{n-1} \frac{\partial}{\partial x}\theta_{t_k}(X_{t_k}) \cdot \Delta X_{t_k} \;- \sum_{k=0}^{n-1} \frac{1}{2}\Big(\Delta X_{t_k} \cdot \frac{\partial}{\partial x}\Big)\Big(\Delta X_{t_k} \cdot \frac{\partial}{\partial x}\big(\theta_{t_k}(X_{t_k})\big)\Big) \qquad (58)\\
&\qquad\qquad - \sum_{k=0}^{n-1} \frac{1}{2}\big((\Delta X_{t_k} \cdot \frac{\partial}{\partial x})\Delta X_{t_k}\big) \cdot \frac{\partial}{\partial x}\big(\theta_{t_k}(X_{t_k})\big) + \circ(\big\langle X\big\rangle_t, 1).
\end{aligned}$$

hence:

$$(58) \xrightarrow{n\to\infty} (\text{TVF}),$$
$$\textit{Right-hand term of } (58) \xrightarrow{n\to\infty} \mathbb{D}_t$$

After proving this Proposition we will focus on the last right-hand term of (58):

$$\sum_{k=0}^{n-1} \frac{1}{2}\big((\Delta X_{t_k}\cdot\frac{\partial}{\partial x})\Delta X_{t_k}\big)\cdot\frac{\partial}{\partial x}\big(\theta_{t_k}(X_{t_k})\big) \ \ (\textbf{discretized modified advection})$$

and prove that it gives rises to the modified advection of section 3, which we recall is:

$$u^* - u^\dagger = \frac{1}{2}\nabla\cdot a - \frac{1}{2}\big(\sigma^T(\nabla\cdot\sigma)\big)^T.$$

Taken together, this will prove the convergence of a new discretization of material derivative $\mathbb{D}_t$:

Proposition 7. *Discretization of the stochastic material derivative*

$$\sum_{k=0}^{n-1}\frac{\partial}{\partial x}\theta_{t_k}(X_{t_k})\cdot\Delta X_{t_k} - \sum_{k=0}^{n-1}\frac{1}{2}\big(\Delta X_{t_k}\cdot\frac{\partial}{\partial x}\big)\Big(\Delta X_{t_k}\cdot\frac{\partial}{\partial x}\big(\theta_{t_k}(X_{t_k})\big)\Big) \xrightarrow{n\to\infty} \mathbb{D}_t + ((u^*-u^\dagger)\mathrm{d}t\cdot\nabla).$$

We now turn to the proof of Proposition 6, which comprises Proposition 8 and Proposition 9. These involve reformulating the second-order components of (56) and (**cross term**), respectively, into a form of (**double advection**).

C.1.2 The Taylor quadratic remainder as a double advection

We first focus on the reformulation of the second order component of (56), so as to introduce the (**double advection**):

Proposition 8. *The* (**quadratic term**) *and the* (**double advection**) *are related in the following way:*

$$\sum_{k=0}^{n-1}\Big(\int_0^1 \frac{\partial^2}{\partial x^2}\theta_{t_{k+1}}(X_{t_k}+\alpha\Delta X_{t_k})(1-\alpha)\mathrm{d}\alpha\Big) : \Delta X_{t_k}\otimes\Delta X_{t_k} =$$
$$\sum_{k=0}^{n-1}\frac{1}{2}\Big(\Delta X_{t_k}\cdot\frac{\partial}{\partial x}\Big)\Big(\Delta X_{t_k}\cdot\frac{\partial}{\partial x}\big(\theta_{t_k}(X_{t_k})\big)\Big) - \sum_{k=0}^{n-1}\frac{1}{2}\Big(\big(\Delta X_{t_k}\cdot\frac{\partial}{\partial x}\big)\Delta X_{t_k}\Big)\cdot\frac{\partial}{\partial x}\Big(\theta_{t_k}\big(X_{t_k}\big)\Big) + \circ\big(\big\langle X\big\rangle_t\big).$$

Lemma 10. *We may rewrite the quadratic remainder term of the Taylor expansion of θ with integral remainder as:*

$$\sum_{k=0}^{n-1}\Big(\int_0^1 \frac{\partial^2}{\partial x^2}\theta_{t_{k+1}}(X_{t_k}+\alpha\Delta X_{t_k})(1-\alpha)\mathrm{d}\alpha\Big) : \Delta X_{t_k}\otimes\Delta X_{t_k} = \sum_{k=0}^{n-1}\frac{1}{2}\frac{\partial^2}{\partial x^2}\theta_{t_k}(X_{t_k}) : \Delta X_{t_k}\otimes\Delta X_{t_k} + \circ\big(\big\langle X\big\rangle_t\big)$$

Proof. First, one has:

$$\sum_{k=0}^{n-1}\Big(\int_0^1 \frac{\partial^2}{\partial x^2}\theta_{t_{k+1}}(X_{t_k}+\alpha\Delta X_{t_k})(1-\alpha)\mathrm{d}\alpha\Big) : \Delta X_{t_k}\otimes\Delta X_{t_k} = \sum_{k=0}^{n-1}\frac{1}{2}\frac{\partial^2}{\partial x^2}\theta_{t_k}(X_{t_k}) : \Delta X_{t_k}\otimes\Delta X_{t_k}$$
$$+\sum_{k=0}^{n-1}\Big(\int_0^1 \big(\frac{\partial^2}{\partial x^2}\theta_{t_{k+1}}(X_{t_k}+\alpha\Delta X_{t_k})-\frac{\partial^2}{\partial x^2}\theta_{t_k}(X_{t_k})\big)(1-\alpha)\mathrm{d}\alpha\Big) : \Delta X_{t_k}\otimes\Delta X_{t_k}.$$

Now let us prove that

$$\sum_{k=0}^{n-1}\Big(\int_0^1 \big(\frac{\partial^2}{\partial x^2}\theta_{t_{k+1}}(X_{t_k}+\alpha\Delta X_{t_k})-\frac{\partial^2}{\partial x^2}\theta_{t_k}(X_{t_k})\big)(1-\alpha)\mathrm{d}\alpha\Big) : \Delta X_{t_k}\otimes\Delta X_{t_k} = \circ(\Delta t).$$

We have:

$$\Big\|\sum_{k=0}^{n-1}\Big(\int_0^1 \big(\frac{\partial^2}{\partial x^2}\theta_{t_{k+1}}(X_{t_k}+\alpha\Delta X_{t_k})-\frac{\partial^2}{\partial x^2}\theta_{t_k}(X_{t_k})\big)(1-\alpha)\mathrm{d}\alpha\Big) : \Delta X_{t_k}\otimes\Delta X_{t_k}\Big\|$$
$$\leq \sum_{k=0}^{n-1}\Big(\int_0^1 \Big\|\big(\frac{\partial^2}{\partial x^2}\theta_{t_{k+1}}(X_{t_k}+\alpha\Delta X_{t_k})-\frac{\partial^2}{\partial x^2}\theta_{t_k}(X_{t_k})\big)\Big\|(1-\alpha)\mathrm{d}\alpha\Big)\|\Delta X_{t_k}\otimes\Delta X_{t_k}\|. \tag{59}$$

Now let us recall that by virtue of definitions 3 and 4:

- $\frac{\partial^2}{\partial x^2}\theta$ is continuous in (t,x),
- X_t is continuous thus uniformly continuous over $[0,T]$,

hence the following estimate for the integrand:

$$\Big\|\big(\frac{\partial^2}{\partial x^2}\theta_{t_{k+1}}(X_{t_k}+\alpha\Delta X_{t_k})-\frac{\partial^2}{\partial x^2}\theta_{t_k}(X_{t_k})\big)\Big\|$$
$$\leq\Big\|\big(\frac{\partial^2}{\partial x^2}\theta_{t_{k+1}}(X_{t_k}+\alpha\Delta X_{t_k})-\frac{\partial^2}{\partial x^2}\theta_{t_{k+1}}(X_{t_k})\big)\Big\|+\Big\|\big(\frac{\partial^2}{\partial x^2}\theta_{t_{k+1}}(X_{t_k})-\frac{\partial^2}{\partial x^2}\theta_{t_k}(X_{t_k})\big)\Big\|$$
$$\leq\frac{1}{2}\Big\|\frac{\partial^2}{\partial x^2}\theta_{\cdot}(\cdot)\Big\|_{C^0}\sup_k\|\Delta X_{t_k}\|+\frac{1}{2}\Big\|\frac{\partial^2}{\partial x^2}\theta_{\cdot}(x)\Big\|_{C^0}\Delta t_k.$$

Including this in (59) we get that

$$\Big\|\sum_{k=0}^{n-1}\Big(\int_0^1 \big(\frac{\partial^2}{\partial x^2}\theta_{t_{k+1}}(X_{t_k}+\alpha\Delta X_{t_k})-\frac{\partial^2}{\partial x^2}\theta_{t_k}(X_{t_k})\big)(1-\alpha)\mathrm{d}\alpha\Big) : \Delta X_{t_k}\otimes\Delta X_{t_k}\Big\|$$
$$\leq \frac{1}{2}\Big(\Big\|\frac{\partial^2}{\partial x^2}\theta_{\cdot}(\cdot)\Big\|_{C^0}\sup_k\|\Delta X_{t_k}\|+\Big\|\frac{\partial^2}{\partial x^2}\theta_{\cdot}(x)\Big\|_{C^0}\Delta t_k\Big)\sum_{k=0}^{n-1}\|\Delta X_{t_k}\otimes\Delta X_{t_k}\|.$$

Adding to the above properties that, per definition 4, X_t is a square integrable martingale, we get our desired result. □

This result leads us to study the following term:

$$\sum_{k=0}^{n-1} \frac{1}{2} \frac{\partial^2}{\partial x^2} \theta_{t_k}(X_{t_k}) : \Delta X_{t_k} \otimes \Delta X_{t_k}. \qquad \textbf{(discretized quadratic term)}$$

We shall seek to draw a bridge between the (**discretized quadratic term**) term and our (**double advection**) term:

$$\sum_{k=0}^{n-1} \frac{1}{2} \frac{\partial^2}{\partial x^2} \theta_{t_k}(X_{t_k}) : \Delta X_{t_k} \otimes \Delta X_{t_k} \implies \sum_{k=0}^{n-1} \frac{1}{2} \Big(\Delta X_{t_k} \cdot \frac{\partial}{\partial x} \Big) \Big(\Delta X_{t_k} \cdot \frac{\partial}{\partial x} \big(\theta_{t_k}(X_{t_k}) \big) \Big). \tag{60}$$

There will be two steps on our transformation of the (**discretized quadratic term**) to the (**double advection**): in a first Lemma we shall bridge the gap between the two components with a remainder term that, as we will show in a second result, can be written as a modified advection.

Lemma 11. *At the discrete level the* (**discretized quadratic term**) *leads to the* (**double advection**) *thus:*

$$\begin{aligned} \sum_{k=0}^{n-1} \frac{1}{2} \frac{\partial^2}{\partial x^2} \theta_{t_k}(X_{t_k}) : \Delta X_{t_k} \otimes \Delta X_{t_k} = & \sum_{k=0}^{n-1} \frac{1}{2} \big(\Delta X_{t_k} \cdot \frac{\partial}{\partial x} \big) \Big(\Delta X_{t_k} \cdot \frac{\partial}{\partial x} \big(\theta_{t_k}(X_{t_k}) \big) \Big) \\ & - \sum_{k=0}^{n-1} \frac{1}{2} \big((\Delta X_{t_k} \cdot \frac{\partial}{\partial x}) \Delta X_{t_k} \big) \cdot \frac{\partial}{\partial x} (\theta_{t_k}(X_{t_k})) \end{aligned}$$

Proof. To prove this integration by-part result we start from the first right-hand term:

$$\begin{aligned} \sum_{k=0}^{n-1} \frac{1}{2} \big(\Delta X_{t_k} \cdot \frac{\partial}{\partial x} \big) \Big(\Delta X_{t_k} \cdot \frac{\partial}{\partial x} \big(\theta_{t_k}(X_{t_k}) \big) \Big) &= \sum_{k=0}^{n-1} \frac{1}{2} \sum_{i,l=1}^{d} (\Delta X^i_{t_k} \frac{\partial}{\partial x^i}) \Big((\Delta X^l_{t_k} \frac{\partial}{\partial x^l}) (\theta_{t_k}(X_{t_k})) \Big) \\ &= \sum_{k=0}^{n-1} \frac{1}{2} \sum_{i,l=1}^{d} \Delta X^i_{t_k} \Delta X^l_{t_k} \frac{\partial^2}{\partial x^i \partial x^l} \theta_{t_k}(X_{t_k}) + \Big(\Delta X^i_{t_k} \big(\frac{\partial}{\partial x^i} \Delta X^l_{t_k} \big) \frac{\partial}{\partial x^l} \Big) \theta_{t_k}(X_{t_k}) \\ &= \sum_{k=0}^{n-1} \frac{1}{2} \frac{\partial^2}{\partial x^2} \theta_{t_k}(X_{t_k}) : \Delta X_{t_k} \otimes \Delta X_{t_k} + \sum_{k=0}^{n-1} \frac{1}{2} \Big(\big(\Delta X_{t_k} \cdot \frac{\partial}{\partial x} \big) \Delta X_{t_k} \Big) \cdot \frac{\partial}{\partial x} \big(\theta_{t_k}(X_{t_k}) \big). \end{aligned}$$

□

Taken together Lemma 10 and 11 yield Proposition 8. We now turn to the reformulation of the (**cross term**).

C.1.3 The (cross term) as a double advection term

While the proof of proposition (8) relied on the (**quadratic term**) and (**double advection**) being both of second order, Proposition 9 will revolve around injecting in the (**cross term**) the conservation of θ, (5), which is at the root of the LU formalism:

Proposition 9. *[Link between the* (**cross term**) *and the* (**double advection**)*]*
There is an equivalency relation between (**cross term**) *and the* (**double advection**)*:*

$$\sum_{k=0}^{n-1}\Big(\frac{\partial}{\partial x}\theta_{t_{k+1}}(X_{t_k})-\frac{\partial}{\partial x}\theta_{t_k}(X_{t_k})\Big)\cdot\Delta X_{t_k}=-\sum_{k=0}^{n-1}\Big(\Delta X_{t_k}\cdot\frac{\partial}{\partial x}\Big)\Big(\Delta X_{t_k}\cdot\frac{\partial}{\partial x}\big(\theta_{t_k}(X_{t_k})\big)\Big)+\circ(1)$$

Proof. Given the semi-martingale writing (1) and (5) of X_t and θ_t, respectively, we obtain directly the following expression for the (**cross term**):

$$\sum_{k=0}^{n-1}\Big(\frac{\partial}{\partial x}\theta_{t_{k+1}}(X_{t_k})-\frac{\partial}{\partial x}\theta_{t_k}(X_{t_k})\Big)\cdot\Delta X_{t_k}\xrightarrow{n\to\infty}\int_0^T\sum_{i=1}^d\mathrm{d}\Big\langle\frac{\partial}{\partial x_i}\theta(X),X^i\Big\rangle_t=-\int_0^T\sigma\frac{\partial}{\partial x}\Big((\sigma\cdot\frac{\partial}{\partial x})\theta_t\Big)\mathrm{d}t.$$

On the other hand:

$$\sum_{k=0}^{n-1}\Big(\Delta X_{t_k}\cdot\frac{\partial}{\partial x}\Big)\Big(\Delta X_{t_k}\cdot\frac{\partial}{\partial x}\big(\theta_{t_k}(X_{t_k})\big)\Big)\xrightarrow{n\to\infty}\int_0^T\sigma\frac{\partial}{\partial x}\Big((\sigma\cdot\frac{\partial}{\partial x})\theta_t\Big)\mathrm{d}t$$

□

Propositions 8 and 9 taken together prove Proposition 6. We will deal now with the remainder in the expansion of Proposition 6, the (**discretized modified advection**).

C.1.4 Convergence of the (discretized modified advection)

Proposition 10. *[Convergence of the* (**discretized modified advection**) *]*
Taking into account the semi-martingale formulation of X_t (1), we obtain:

$$\sum_{k=0}^{n-1}\frac{1}{2}\Big(\Big(\Delta X_{t_k}\cdot\frac{\partial}{\partial x}\Big)\Delta X_{t_k}\Big)\cdot\frac{\partial}{\partial x}\big(\theta_{t_k}(X_{t_k})\big)=\sum_{k=0}^{n-1}\frac{1}{2}\Big(\Big((\nabla\cdot a)-\big(\sigma^T(\nabla\cdot\sigma)\big)^T\Big)\cdot\nabla\Big)\theta_{t_k}+\circ(1).\tag{61}$$

Proof. Our analysis begins with a convergence result based on the formulation of X_t (1), followed by a vector analysis result that will lead to our conclusion. First, let us prove that:

$$\sum_{k=0}^{n-1}\frac{1}{2}\Big(\big(\Delta X_{t_k}\cdot\frac{\partial}{\partial x}\big)\Delta X_{t_k}\Big)\cdot\frac{\partial}{\partial x}\big(\theta_{t_k}(X_{t_k})\big)=\sum_{k=0}^{n-1}\frac{1}{2}\Big(\big(\sigma\Delta B_{t_k}\cdot\frac{\partial}{\partial x}\big)\sigma\Delta B_{t_k}\Big)\cdot\frac{\partial}{\partial x}\big(\theta_{t_k}\big)+\circ(1).$$

Given the semi-martingale writing of X_t this amounts to proving:

$$\sum_{k=0}^{n-1}\frac{1}{2}\Big(\big(u\Delta t_k\cdot\frac{\partial}{\partial x}\big)u\Delta t_k\Big)\cdot\frac{\partial}{\partial x}\big(\theta_{t_k}(X_{t_k})\big)\xrightarrow{n\to\infty}0$$

$$\sum_{k=0}^{n-1}\frac{1}{2}\Big(\big(\sigma\Delta B_{t_k}\cdot\frac{\partial}{\partial x}\big)u\Delta t_k\Big)\cdot\frac{\partial}{\partial x}\big(\theta_{t_k}\big)\xrightarrow{n\to\infty}0$$

$$\sum_{k=0}^{n-1}\frac{1}{2}\Big(\big(u\Delta t_k\cdot\frac{\partial}{\partial x}\big)\sigma\Delta B_{t_k}\Big)\cdot\frac{\partial}{\partial x}\big(\theta_{t_k}\big)\xrightarrow{n\to\infty}0$$

Here again, we suppose, for sake of simplicity that $\Delta t_k = \Delta t$. For the first term we get

$$\sum_{k=0}^{n-1} \frac{1}{2}\Big((u\Delta t_k \cdot \frac{\partial}{\partial x})u\Delta t_k\Big) \cdot \frac{\partial}{\partial x}(\theta_{t_k}) = \Delta t \underbrace{\sum_{k=0}^{n-1} \frac{1}{2}\Big((u\Delta t_k \cdot \frac{\partial}{\partial x})u\Big) \cdot \frac{\partial}{\partial x}(\theta_{t_k})}_{\substack{\xrightarrow{n\to\infty} \int_0^T \frac{1}{2}\left((u\cdot\frac{\partial}{\partial x})u\right)\cdot\frac{\partial}{\partial x}(\theta_t)\mathrm{d}t \\ Riemann \\ integral}},$$

hence our result. As for the second and third term :

$$\sum_{k=0}^{n-1} \frac{1}{2}\Big((\sigma\Delta B_{t_k} \cdot \frac{\partial}{\partial x})u\Delta t_k\Big) \cdot \frac{\partial}{\partial x}(\theta_{t_k}) = \Delta t \underbrace{\sum_{k=0}^{n-1} \frac{1}{2}\Big((\sigma\Delta B_{t_k} \cdot \frac{\partial}{\partial x})u\Big) \cdot \frac{\partial}{\partial x}(\theta_{t_k})}_{\substack{\xrightarrow{n\to\infty} \int_0^T \frac{1}{2}\left((\sigma\mathrm{d}B_t\cdot\frac{\partial}{\partial x})u\right)\cdot\frac{\partial}{\partial x}(\theta_t) \\ Ito \\ integral}},$$

and

$$\sum_{k=0}^{n-1} \frac{1}{2}\Big((u\Delta t_k \cdot \frac{\partial}{\partial x})\sigma\Delta B_{t_k}\Big) \cdot \frac{\partial}{\partial x}(\theta_{t_k}) = \Delta t \underbrace{\sum_{k=0}^{n-1} \frac{1}{2}\Big((u \cdot \frac{\partial}{\partial x})\sigma\Delta B_{t_k}\Big) \cdot \frac{\partial}{\partial x}(\theta_{t_k})}_{\substack{\xrightarrow{n\to\infty} \int_0^T \frac{1}{2}\left((u\cdot\frac{\partial}{\partial x})\sigma\mathrm{d}B_t\right)\cdot\frac{\partial}{\partial x}(\theta_t) \\ Ito \\ integral}}.$$

Now let us reformulate the right-hand term of (61) in a discrete-time equivalent of the proof of lemma 3. Namely, we have:

$$\begin{aligned}\sum_{k=0}^{n-1} \frac{1}{2}\Big((\sigma\Delta B_{t_k} \cdot \frac{\partial}{\partial x})\sigma\Delta B_{t_k}\Big) \cdot \frac{\partial}{\partial x}(\theta_{t_k}) &= \sum_{k=0}^{n-1} \frac{1}{2} \sum_{i,j,l=1}^{d} \Big(\sigma_{i,j}(\frac{\partial}{\partial x^i}\sigma_{l,j})\frac{\partial}{\partial x^l}\Big)\theta_{t_k} \\ &= \sum_{k=0}^{n-1} \frac{1}{2} \sum_{i,j,l=1}^{d} \Big((\frac{\partial}{\partial x^i}(\sigma_{i,j}\sigma_{l,j}) - (\frac{\partial}{\partial x^i}\sigma_{i,j})\sigma_{l,j})\frac{\partial}{\partial x^l}\Big)\theta_k.\end{aligned}$$

Using vector notation, this means:

$$\sum_{k=0}^{n-1} \frac{1}{2}\Big((\sigma : \nabla\sigma^T) \cdot \nabla\Big)\theta_{t_k} = \sum_{k=0}^{n-1} \frac{1}{2}\Big(\Big((\nabla \cdot a) - \big(\sigma^T(\nabla \cdot \sigma)\big)^T\Big) \cdot \nabla\Big)\theta_{t_k}$$

Thus we do have the required form for our remainder term, hence our result. □

Taken together Propositions 8, 9 and 10 lead to Proposition 7. We now turn to the second interpretation of our double iterated schemes.

C.2 The Milstein interpretation

The purpose of this part is to frame the schemes of subsection 3.5 under what we will call a Milstein scheme interpretation of the stochastic partial differential

(3) which we recall here:

$$\partial_t U_t + f\big[\big((u-u^*)\mathrm{d}t + \sigma \mathrm{d}B_t\big)\big](U_t) - \frac{1}{2}\nabla\cdot\big(a\nabla U_t\big)\mathrm{d}t = 0. \tag{62}$$

In the following, we will first unfold a second order expansion of our SPDE which will make iterated stochastic integrals appear. We will then re-formulate those integrals which will lead us to the Milstein scheme before writing it in the context of LU and prove, under one hypothesis on the noise, that the schemes of subsection 3.5 are consistent with this interpretation. Before proceeding we set the framework for the considerations of this section; we start by recasting (62) under generic form:

$$\partial_t \theta_t + f\big[\big((u-u^*)\mathrm{d}t + \sigma \mathrm{d}B_t\big)\big](\theta_t) - \frac{1}{2}\nabla\cdot(a\nabla\theta_t)\mathrm{d}t = 0. \tag{63}$$

Before further exploring this Milstein scheme interpretation, let us try to get a more precise understanding of the context at hand.

Remark 9. *The equation* (63) *on* θ_t*, was obtained after applying the Ito-Wentzell (total variation) formula* (TVF)*, which draws the bridge between the* ***Lagrangian framework*** *and the* ***Eulerian framework****. In that framework* θ_t *was a functionnal over* t *and stochastic process* X_t *which was the variable over* $\mathcal{S}$*.*

In the following part we will consider (63) *as a dynamical system over* θ_t *is a stochastic process with values in the* ***Eulerian*** *fields over domain* $\mathcal{S}$ *with* X_t *becoming the main "drive" of the evolution of* θ_t*.*

As the variable θ_t *is now a time-only stochastic process with values in vector fields, we may now write:*

$$\partial_t \theta_t = \mathrm{d}_t \theta_t.$$

Heeding the considerations of remark 9, we now rewrite (63) as:

$$\mathrm{d}_t\theta_t = \alpha(t,\theta_t)\mathrm{d}t + (\sigma_t \mathrm{d}B_t\cdot\nabla)\theta, \tag{64}$$

where we have gathered the bounded variation and martingale parts of our process as:

$$\alpha(t,\theta)\mathrm{d}t = f\big[(u-u^*)\mathrm{d}t\big](\theta) - \frac{1}{2}\nabla\cdot(a\nabla\theta)\mathrm{d}t, \tag{65}$$

Furthermore we may apply the Milstein framework in the case of a noise expressed on a finite number of modes alone: we recall that initially the noise structure is expressed as (2) that is

$$\sigma_t\, B_t = \sum_{\kappa=0}^{\infty} \phi_\kappa(t)\, \beta_t^\kappa,$$

where the $\phi_\kappa(t)$ are the time dependant eigenvectors of σ_t; in particular they are scalar fields over $\mathcal{S}$; now, in this section, we shall consider:

$$\sigma_t\, B_t = \sum_{\kappa=0}^{N} \phi_\kappa(t)\, \beta_t^\kappa,$$

thus giving us the following noise structure:

$$\sigma_t \, \mathrm{d}B_t = \sum_{\kappa=0}^{N} \phi_\kappa(t) \, \mathrm{d}\beta_t^\kappa. \tag{66}$$

We now take to the study of the induced Milstein scheme.

C.2.1 Second order expansion of a stochastic differential equation

We shall deal here with a particular case of the Milstein expansions which allows for a broader framework than the classical one. For a more complete analysis of the Milstein scheme we refer to chapter 5 of (Kloeden and Platen, 1999). In integral form (64) becomes:

$$\theta_t = \theta_s + \int_s^t \alpha(\tau, \theta_\tau)\mathrm{d}\tau + \int_s^t (\sigma_t \mathrm{d}B_\tau \cdot \nabla)\theta_\tau. \tag{67}$$

We will now provide an expansion of the last right-hand term in order to introduce the Milstein scheme.

Lemma 12. *The martingale component of* (67) *can be expanded w.r.t* t *and then* θ *as:*

$$\int_s^t (\sigma_\tau \mathrm{d}B_\tau \cdot \nabla)\theta_\tau = \int_s^t (\sigma_s \mathrm{d}B_\tau \cdot \nabla)\theta_s - \int_s^t \big(\sigma_s \mathrm{d}B_\tau \cdot \nabla\big)\big(\int_s^\tau (\sigma_s \mathrm{d}B_{\tau'} \cdot \nabla)\theta_s\big) + H.O.T.$$

Proof. We unfold our expansion first w.r.t t:

$$\int_s^t (\sigma_\tau \mathrm{d}B_\tau \cdot \nabla)\theta_\tau = \int_s^t (\sigma_s \mathrm{d}B_\tau \cdot \nabla)\theta_\tau + \int_s^t \big(\int_s^\tau \frac{\partial \sigma}{\partial t} \mathrm{d}\tau' \mathrm{d}B_\tau \cdot \nabla\big)\theta_\tau,$$

and notice that:

$$\Big\| \int_s^t \big(\int_s^\tau \frac{\partial \sigma}{\partial t} \mathrm{d}\tau' \mathrm{d}B_\tau \cdot \nabla\big)\theta_\tau \Big\| \leq \Big\| \frac{\partial \sigma}{\partial t} \Big\|_{C^0} \Big\| \theta \Big\|_{C^0} \Big\| \int_s^t \int_s^\tau \mathrm{d}\tau' \mathrm{d}B_\tau \Big\| = \circ(t-s),$$

hence:

$$\int_s^t (\sigma_\tau \mathrm{d}B_\tau \cdot \nabla)\theta_\tau = \int_s^t (\sigma_s \mathrm{d}B_\tau \cdot \nabla)\theta_\tau + H.O.T.$$

Now taking into account this result we follow up with an expansion w.r.t θ:

$$\begin{aligned}
\int_s^t (\sigma_s \mathrm{d}B_\tau \cdot \nabla)\theta_\tau &= \int_s^t (\sigma_s \mathrm{d}B_\tau \cdot \nabla)\theta_s + \int_s^t (\sigma_s \mathrm{d}B_\tau \cdot \nabla)\big(\theta_\tau - \theta_s\big) \\
&= \int_s^t (\sigma_s \mathrm{d}B_\tau \cdot \nabla)\theta_s - \int_s^t \big(\sigma_s \mathrm{d}B_\tau \cdot \nabla\big)\big(\int_s^\tau a(\tau', \theta_{\tau'})\mathrm{d}\tau'\big) \\
&\quad - \int_s^t \big(\sigma_s \mathrm{d}B_\tau \cdot \nabla\big)\big(\int_s^\tau (\sigma_s \mathrm{d}B_{\tau'} \cdot \nabla)\theta_{\tau'}\big).
\end{aligned}$$

Including the structure of the noise in the second right-hand term we get:

$$\int_s^t \big(\sigma_s \mathrm{d}B_\tau \cdot \nabla\big)\big(\int_s^\tau \alpha(\tau', \theta_{\tau'})\mathrm{d}\tau'\big) = \int_s^t \sum_{\kappa=0}^N \phi_\kappa(s)\cdot\nabla\big(\int_s^\tau \alpha(\tau', \theta_{\tau'})\mathrm{d}\tau'\big)\mathrm{d}\beta_\tau^\kappa$$
$$= \circ(t-s) = H.O.T,$$

thus

$$\int_s^t (\sigma_s \mathrm{d}B_\tau \cdot \nabla)\theta_\tau = \int_s^t (\sigma_s \mathrm{d}B_\tau \cdot \nabla)\theta_s - \int_s^t \big(\sigma_s \mathrm{d}B_\tau \cdot \nabla\big)\big(\int_s^\tau (\sigma_s \mathrm{d}B_{\tau'} \cdot \nabla)\theta_{\tau'}\big) + H.O.T.$$

By reiterating our reasoning on $\theta_{\tau'}$ and truncating high order terms we get the desired result. □

The expansion of the bounded variation component of θ_t is more straightforward:

$$\int_s^t \alpha(\tau, \theta_\tau)\mathrm{d}\tau = \int_s^t \alpha(s, \theta_s)\mathrm{d}\tau + H.O.T,$$

hence the following result:

Proposition 11. *Formula* (67) *has the following expansion:*

$$\theta_t = \theta_s + \int_s^t \alpha(s, \theta_s)\mathrm{d}\tau + \int_s^t (\sigma_s \mathrm{d}B_\tau \cdot \nabla)\theta_s - \int_s^t \big(\sigma_s \mathrm{d}B_\tau \cdot \nabla\big)\big(\int_s^\tau (\sigma_s \mathrm{d}B_{\tau'} \cdot \nabla)\theta_s\big) + H.O.T. \tag{68}$$

Neglecting the higher order terms give rises to the Milstein scheme, the main issue of which, is the iterated stochastic integral. We shall now focus on this later component and its parenthood to the quadratic term of the Itô Wentzell formula.

C.2.2 Treatment of the iterated integral and Milstein scheme

We now focus on the last right-hand term component of (68) which we rewrite:

$$\int_s^t (\sigma_s \mathrm{d}B_\tau \cdot \nabla)\Big(\int_s^\tau (\sigma_s \mathrm{d}B_{\tau'} \cdot \nabla)\theta_s\Big) = \sum_{\kappa=0}^N \sum_{\kappa'=0}^N \int_s^t \Big(\phi_\kappa(s)\cdot\nabla\Big)\Big(\int_s^\tau \big(\phi_{\kappa'}(s)\cdot\nabla\big)\theta_s\big)\mathrm{d}\beta_{\tau'}^{\kappa'}\Big)\mathrm{d}\beta_\tau^\kappa$$
$$= \sum_{\kappa=0}^N \sum_{\kappa'=0}^N \Big(\phi_\kappa(s)\cdot\nabla\Big)\Big(\big(\phi_{\kappa'}(s)\cdot\nabla\big)\theta_s\Big)\int_s^t \int_s^\tau \mathrm{d}\beta_{\tau'}^{\kappa'}\mathrm{d}\beta_\tau^\kappa.$$

Thus to reach a fully explicit Milstein scheme, we have to compute $\int_s^t \int_s^\tau \mathrm{d}\beta_{\tau'}^{\kappa'}\mathrm{d}\beta_\tau^\kappa$, which we do in the following lemma:

Lemma 13. *Let B_t be for a d-dimensionnal Brownian motion; then:*

$$\int_s^t \int_s^\tau \mathrm{d}\beta_{\tau'}^{\kappa'}\mathrm{d}\beta_\tau^\kappa = (\beta_t^\kappa - \beta_s^\kappa)(\beta_t^{\kappa'} - \beta_s^{\kappa'}) - \frac{1}{2}\delta_{\kappa=\kappa'}(t-s) + \frac{1}{2}\mathcal{A}(\beta^\kappa, \beta^{\kappa'}),$$

where

$$\mathcal{A}(\beta^\kappa, \beta^{\kappa'}) := \Big(\int_s^t \int_s^\tau d\beta_{\tau'}^{\kappa'} \mathrm{d}\beta_\tau^\kappa - \int_s^t \int_s^\tau \mathrm{d}\beta_{\tau'}^\kappa d\beta_\tau^{\kappa'} \Big),$$

is the Levy area.

Proof. Let us start by writing the following Ito expansion:

$$\mathrm{d}\big((\beta_r^{\kappa'} - \beta_s^{\kappa'})(\beta_r^\kappa - \beta_s^\kappa)\big) = (\beta_r^{\kappa'} - \beta_s^{\kappa'})\mathrm{d}\beta_r^\kappa + (\beta_r^\kappa - \beta_s^\kappa)\mathrm{d}\beta_r^{\kappa'} + \mathrm{d}\big\langle \beta^\kappa, \beta^{\kappa'} \big\rangle_r.$$

Therefore decomposing $\int_s^t \int_s^\tau \mathrm{d}\beta_{\tau'}^{\kappa'} \mathrm{d}\beta_\tau^\kappa$ into symmetrical and anti-symmetrical parts we have:

$$\begin{aligned}
\int_s^t \int_s^\tau \mathrm{d}\beta_{\tau'}^{\kappa'} \mathrm{d}\beta_\tau^\kappa =& \frac{1}{2}\Big(\int_s^t (\beta_\tau^{\kappa'} - \beta_s^{\kappa'})\mathrm{d}\beta_\tau^\kappa + \int_s^t (\beta_\tau^\kappa - \beta_s^\kappa)\mathrm{d}\beta_\tau^{\kappa'} \Big) \\
&+ \frac{1}{2}\Big(\int_s^t \int_s^\tau \mathrm{d}\beta_{\tau'}^{\kappa'} \mathrm{d}\beta_\tau^\kappa - \int_s^t \int_s^\tau \mathrm{d}\beta_{\tau'}^\kappa \mathrm{d}\beta_\tau^{\kappa'} \Big) \\
=& \frac{1}{2}\big((\beta_t^{\kappa'} - \beta_s^{\kappa'})(\beta_t^\kappa - \beta_s^\kappa) - \delta_{\kappa=\kappa'}(t-s) \big) + \frac{1}{2}\mathcal{A}(\beta^{\kappa'}, \beta^\kappa)
\end{aligned}$$

□

Now, including Lemma 13 in (68) yields the following scheme.

Definition 8. *The Milstein scheme expansion reads as:*

$$\begin{aligned}
\theta_t = \theta_s + \int_s^t \alpha(s, \theta_s)\mathrm{d}\tau + \int_s^t (\sigma_s \mathrm{d}B_\tau \cdot \nabla)\theta_s - \sum_{\kappa=0}^{N} \sum_{\kappa'=0}^{N} \Big(\phi_\kappa(s) \cdot \nabla \Big) \Big(\big(\phi_{\kappa'}(s) \cdot \nabla \big) \theta_s \Big) \\
\frac{1}{2}\Big((\beta_t^\kappa - \beta_s^\kappa)(\beta_t^{\kappa'} - \beta_s^{\kappa'}) - \delta_{\kappa=\kappa'}(t-s) + \mathcal{A}(\beta^\kappa, \beta^{\kappa'}) \Big), \quad (69)
\end{aligned}$$

In the next section, we apply this setting to our case (63).

C.2.3 Milstein equation in the LU context

The main objective of this section is to replace the generic form (64) by the differential form obtained in the LU framework (63) to build a Milstein integration scheme within the LU framework. However, before doing so, we introduce a simplifying statement to our treatment of the Milstein scheme in the LU case.

Hypothesis 1. In the case of fluid dynamics under the LU framework, the noise (66) is considered to be of zero Levy area i.e :

$$\mathcal{A}(\beta^\kappa, \beta^{\kappa'}) \equiv 0$$

The hypothesis is supported by numerical results presented in (Boulvard and Mémin, 2024), which highlight the effectiveness of modeling sub-grid variability with a Wiener process while maintaining a negligible Lévy area, consistent with high resolution data fluctuations. Applying the Milstein scheme under this hypothesis to (63), we obtain:

Proposition 12. *A Milstein scheme on* (63) *under hypothesis 1 reads as:*

$$\theta_{t+\Delta t} = \theta_t + f\Big[\big(u - (u^* - u^\dagger)\big)\Delta t + \sigma\Delta B_t\Big](\theta) - \frac{1}{2}\big(\sigma\Delta B_t \cdot \nabla\big)\big((\sigma\Delta B_t \cdot \nabla)\theta\big).$$

Proof. Here, going back to our initial framework we slightly adapt our notations:

$$[s;t] \mapsto [t;t+\Delta t].$$

Now applying hypothesis (1) reduces our expansion to:

$$\begin{aligned}\theta_{t+\Delta t} = \theta_t &+ \int_t^{t+\Delta t} \alpha(t,\theta_t)\mathrm{d}\tau + \int_t^{t+\Delta t} (\sigma_t \mathrm{d}B_\tau \cdot \nabla)\theta_t \\ &- \sum_{\kappa=0}^{N}\sum_{\kappa'=0}^{N}\Big(\phi_\kappa(t)\cdot\nabla\Big)\Big(\big(\phi_{\kappa'}(t)\cdot\nabla\big)\theta_t\Big)\frac{1}{2}\Big(\Delta\beta_t^\kappa\Delta\beta_t^{\kappa'} - \delta_{\kappa=\kappa'}\Delta t\Big).\end{aligned}$$

We then rewrite the first bilinear term as:

$$\sum_{\kappa=0}^{N}\sum_{\kappa'=0}^{N}\Big(\phi_\kappa(t)\cdot\nabla\Big)\Big(\big(\phi_{\kappa'}(t)\cdot\nabla\big)\theta_t\Big)\Big)\Delta\beta_t^\kappa\Delta\beta_t^{\kappa'} = \big(\sigma\Delta B_t\cdot\nabla\big)\big((\sigma\Delta B_t\cdot\nabla)\theta\big)$$

As for the remaining bilinear term, it reads:

$$\sum_{\kappa=0}^{N}\sum_{\kappa'=0}^{N}\Big(\phi_\kappa(t)\cdot\nabla\big)\big((\phi_{\kappa'}(t)\cdot\nabla)\theta_t\big)\Big)\delta_{\kappa=\kappa'} = \sum_{\kappa=0}^{N}\big(\phi_\kappa(t)\cdot\nabla\big)\big((\phi_\kappa(t)\cdot\nabla)\theta_t\big),$$

moreover using the same computations as in Lemma 6 we may write:

$$\sum_{\kappa=0}^{N}\big(\phi_\kappa(t)\cdot\nabla\big)\big((\phi_\kappa(t)\cdot\nabla)\theta_t\big) = \nabla\cdot(a\nabla\theta_t) - \Big(\Big(\big(\sigma^T(\nabla\cdot\sigma)\big)^T\Big)\cdot\nabla\Big)\theta_t$$

thus,

$$\begin{aligned}&\sum_{\kappa=0}^{N}\sum_{k'=0}^{N}\Big(\phi_\kappa(t)\cdot\nabla\Big)\Big(\big(\phi_{\kappa'}(t)\cdot\nabla\big)\theta_t\Big)\frac{1}{2}(\Delta\beta_t^\kappa\Delta\beta_t^{\kappa'} - \delta_{\kappa=\kappa'}\Delta t) \\ &= \frac{1}{2}\big(\sigma\Delta B_t\cdot\nabla\big)\big((\sigma\Delta B_t\cdot\nabla)\theta\big) - \frac{1}{2}\Big(\nabla\cdot(a\nabla\theta_t) - \Big(\big(\sigma^T(\nabla\cdot\sigma)\big)^T\cdot\nabla\Big)\theta_t\Big)\Delta t.\end{aligned}$$

Therefore the Milstein expansion in the LU case is:

$$\theta_{t+\Delta t} = \theta_t + \int_t^{t+\Delta t} f\big[\big(u-(u^*-u^\dagger)\big)\mathrm{d}\tau + \sigma\mathrm{d}B_\tau\big](\theta) - \frac{1}{2}(\sigma\Delta B_t\cdot\nabla)\big((\sigma\Delta B_t\cdot\nabla)\theta\big).$$

□

Proposition 12, in conjunction with Proposition 3, proves that the schemes of subsection 3.5 are consistent with the Milstein interpretation of our stochastic Saint-Venant equations (62).

Remark 10. *The Milstein scheme* (69) *yields a second-order term in the following form:*

$$\sum_{\kappa=0}^{N}\sum_{\kappa'=0}^{N}\big(\phi_\kappa(t)\cdot\nabla\big)\big((\phi_{\kappa'}(t)\cdot\nabla)\theta_t\big)\frac{1}{2}\big(\Delta\beta_t^\kappa\Delta\beta_t^{\kappa'}-\delta_{\kappa=\kappa'}\Delta t+\mathcal{A}(\beta^\kappa,\beta^{\kappa'})\big).$$

We observe the convergence of

$$\sum_{\kappa=0}^{N}\sum_{\kappa'=0}^{N}\bigg(\Big(\phi_\kappa(t)\cdot\nabla\Big)\Big((\phi_{\kappa'}(t)\cdot\nabla)\theta_t\Big)\bigg)\frac{1}{2}\Delta\beta_t^\kappa\Delta\beta_t^{\kappa'}\to\sum_{\kappa=0}^{N}\sum_{\kappa'=0}^{N}\Big(\phi_\kappa(t)\cdot\nabla\Big)\Big((\phi_{\kappa'}(t)\cdot\nabla)\theta_t\Big)\frac{1}{2}\delta_{\kappa=\kappa'}\Delta t,$$

as the number of steps in the Milstein scheme tends to infinity, mirroring the convergence of (**double advection**) *in Lemma 2 as the number of time steps in the Itô discretization steps tends to infinity. Actually,*

$$\sum_{\kappa=0}^{N}\sum_{\kappa'=0}^{N}\Big(\phi_\kappa(t)\cdot\nabla\Big)\Big((\phi_{\kappa'}(t)\cdot\nabla)\theta_t\Big)\frac{1}{2}\big(\Delta\beta_t^\kappa\Delta\beta_t^{\kappa'}-\delta_{\kappa=\kappa'}\Delta t\big)$$

can be considered as a correction under the double advection form of the Itô-Wentzell formula by the Milstein scheme. This same correction was at play in our study of the discretization of the Itô-Wentzell formula at the beginning of this appendix. So far, the discretized Itô-Wentzell formula interpretation and the Milstein scheme interpretation are consistent. They differ in the presence of an additional correction term, the Levy area:

$$\sum_{\kappa=0}^{N}\sum_{\kappa'=0}^{N}\Big(\phi_\kappa(t)\cdot\nabla\Big)\Big((\phi_{\kappa'}(t)\cdot\nabla)\theta_t\Big)\frac{1}{2}\big(\mathcal{A}(\beta^k,\beta^{k'})\big),$$

which accounts for the geometric correction between a stochastic integral and its discretization. Having neglected it we have made the Milstein scheme interpretation and the discretized Itô-Wentzell formula interpretation fully consistent.

authoryear

References

Bauer, W., Chandramouli, P., Chapron, B., Li, L., Mémin, E., 2020a. Deciphering the role of small-scale inhomogeneity on geophysical flow structuration: A stochastic approach. Journal of Physical Oceanography 50, 983 – 1003.

Bauer, W., Chandramouli, P., Li, L., Mémin, E., 2020b. Stochastic representation of mesoscale eddy effects in coarse-resolution barotropic models. Ocean Modelling 151, 101646.

Boulvard, P.M., Mémin, E., 2024. Diagnostic of the lévy area for geophysical flow models in view of defining high order stochastic discrete-time schemes. Foundations of Data Science 6, 1–21.

Brecht, R., Li, L., Bauer, W., Mémin, E., 2021. Rotating shallow water flow under location uncertainty with a structure-preserving discretization. Journal of Advances in Modeling Earth Systems 13, 1–28.

Bristeau, M.O., Mangeney, A., Sainte-Marie, J., Seguin, N., 2015. An energy-consistent depth-averaged Euler system: Derivation and properties. Discrete and Continuous Dynamical Systems - Series B 20, 961–988. URL: http://aimsciences.org/journals/displayArticlesnew.jsp?paperID=10801, doi:10.3934/dcdsb.2015.20.961.

Brzeżniak, Z., Capinski, M., Flandoli, F., 1991. Stochastic partial differential equations and turbulence. Math. Models Methods Appl. Sci. 1, 41–59.

Chandramouli, P., Heitz, D., Laizet, S., Mémin, E., 2018. Coarse large-eddy simulations in a transitional wake flow with flow models under location uncertainty. Comp. & Fluids 168, 170–189.

Chandramouli, P., Mémin, E., Heitz, D., 2020. 4d large scale variational data assimilation of a turbulent flow with a dynamics error model. Journal of Computational Physics 412, 109446.

Chapron, B., Dérian, P., Mémin, E., Resseguier, V., 2018. Large-scale flows under location uncertainty: a consistent stochastic framework. QJRMS 144, 251–260.

Clement, S., Blayo, E., Debreu, L., Brankart, J.M., Brasseur, P., Li, L., Mémin, E., 2025. Link between stochastic grid perturbation and location uncertainty framework. Journal of Advances in Modeling Earth Systems 17, e2024MS004528.

Cotter, C., Crisan, D., Holm, D., Pan, W., Shevchenko, I., 2019. Numerically modeling stochastic Lie transport in fluid dynamics. SIAM J. on Multiscale Modeling and Simulation 17, 192–232.

Cotter, C.J., Crisan, D., Holm, D.D., Pan, W., Shevchenko, I., 2018. Numerically modelling stochastic lie transport in fluid dynamics. doi:10.48550/ARXIV.1801.09729.

Debussche, A., Hug, B., Mémin, E., 2023. A consistent stochastic large-scale representation of the Navier–Stokes equations. Journal of Mathematical Fluid Mechanics 25, 19.

Debussche, A., Mémin, E., Moneyron, A., 2024a. Derivation of stochastic models for coastal waves, in: Stochastic Transport in Upper Ocean Dynamics III.

Debussche, A., Mémin, É., Moneyron, A., 2024b. Some properties of a non-hydrostatic stochastic oceanic primitive equations model, in: Stochastic Transport in Upper Ocean Dynamics III. URL: https://inria.hal.science/hal-04632530.

Dufée, B., Mémin, E., Crisan, D., 2022. Stochastic parametrization: An alternative to inflation in ensemble Kalman filters. Quarterly Journal of the Royal Meteorological Society 148, 1075–1091. URL: https://doi.org/10.1002/qj.4247, doi:https://doi.org/10.1002/qj.4247.

Dufée, B., Mémin, E., Crisan, D., 2023. Observation-Based Noise Calibration: An Efficient Dynamics for the Ensemble Kalman Filter, in: Stochastic Transport in Upper Ocean Dynamics. Springer International Publishing. volume 10 of *Mathematics of Planet Earth*, pp. 43–56. URL: https://hal.science/hal-03910764, doi:10.1007/978-3-031-18988-3_4.

El Hassanieh, C., Rigal, M., Sainte-Marie, J., 2024. Implicit kinetic schemes for the Saint-Venant system URL: https://hal.science/hal-04048832. working paper or preprint.

Fiorini, C., Boulvard, P.M., Li, L., Mémin, E., 2022. A two-step numerical scheme in time for surface quasi geostrophic equations under location uncertainty.

Fiorini, C., Boulvard, P.M., Li, L., Mémin, E., 2023. A two-step numerical scheme in time for surface quasi geostrophic equations under location uncertainty, in: Chapron, B., Crisan, D., Holm, D., Mémin, E., Radomska, A. (Eds.), Stochastic Transport in Upper Ocean Dynamics, Springer. pp. 57–67.

Flandoli, F., 2011. Random Perturbation of PDEs and Fluid Dynamic Models: École d'été de Probabilités de Saint-Flour XL–2010. volume 2015. Springer Science & Business Media.

Flandoli, F., Pappalettera, U., 2021. 2d euler equations with stratonovich transport noise as a large-scale stochastic model reduction. Journal of Nonlinear Science 31, 24. URL: https://doi.org/10.1007/s00332-021-09681-w, doi:10.1007/s00332-021-09681-w.

Foster, J., Lyons, T., Oberhauser, H., 2020. An optimal polynomial approximation of brownian motion. SIAM Journal on Numerical Analysis 58, 1393–1421.

Galeati, L., Luo, D., 2023. Weak well-posedness by transport noise for a class of 2d fluid dynamics equations. arXiv:2305.08761.

Gerbeau, J.F., Perthame, B., 2001. Derivation of Viscous Saint-Venant System for Laminar Shallow Water; Numerical Validation. Discrete Contin. Dyn. Syst. Ser. B 1, 89–102.

Guermond, J.L., Oden, J.T., Prudhomme, S., 2004. Mathematical perspectives on large eddy simulation models for turbulent flows. Journal of Mathematical Fluid Mechanics 6, 194–248.

Kadri Harouna, S., Mémin, E., 2017. Stochastic representation of the Reynolds transport theorem: revisiting large-scale modeling. Computers & Fluids 156, 456–469. URL: https://hal.inria.fr/hal-01394780, doi:10.1016/j.compfluid.2017.08.017.

Kloeden, P., Platen, E., 1999. Numerical Solution of Stochastic Differential Equations. Springer, Berlin.

Kunita, H., 1990. Stochastic flows and stochastic differential equations. Cambridge University Press.

Lang, O., Crisan, D., Mémin, E., 2023a. Analytical properties for a stochastic rotating shallow water model under location uncertainty. Journal of Mathematical Fluid Mechanics 25, 29.

Lang, O., Crisan, D., Mémin, E., 2023b. Analytical Properties for a Stochastic Rotating Shallow Water Model Under Location Uncertainty. Journal of Mathematical Fluid Mechanics 25, 29. URL: https://hal.inria.fr/hal-03832450, doi:10.1007/s00021-023-00769-9.

Li, L., Deremble, B., Lahaye, N., Mémin, E., 2023. Stochastic Data-Driven Parameterization of Unresolved Eddy Effects in a Baroclinic Quasi-Geostrophic Model. Journal of Advances in Modeling Earth Systems 15.

Majda, A., Timofeyev, I., Eijnden, E.V., 1999. Models for stochastic climate prediction. PNAS .

Mangeney, A., Bouchut, F., Thomas, N., P. Vilotte, J., Bristeau, M.O., 2007. Numerical modeling of self-channeling granular flows and of their levee-channel deposits. Journal of Geophysical Research 112. URL: http://hal.archives-ouvertes.fr/hal-00311797.

Marche, F., 2007. Derivation of a new two-dimensional viscous shallow water model with varying topography, bottom friction and capillary effects. European Journal of Mechanic /B 26, 49–63.

Mémin, E., 2014. Fluid flow dynamics under location uncertainty. Geophys. & Astro. Fluid Dyn. 108, 119–146.

Mémin, E., Li, L., Lahaye, N., Tissot, G., Chapron, B., 2024. Linear wave solutions of a stochastic shallow water model, in: Chapron, B., Crisan, D., Holm, D., Mémin, E., Radomska, A. (Eds.), Stochastic Transport in Upper Ocean Dynamics II, Springer Nature Switzerland, Cham. pp. 223–245.

Pinier, B., Mémin, E., Laizet, S., Lewandowski, R., 2019. Stochastic flow approach to model the mean velocity profile of wall-bounded flows. Phys. Rev. E 99, 063101.

Prato, G.D., Zabczyk, J., 1992. Stochastic equations in infinite dimensions. Cambridge University Press.

Resseguier, V., Li, L., Jouan, G., Dérian, P., Mémin, E., Chapron, B., 2021. New trends in ensemble forecast strategy: Uncertainty quantification for coarse-grid computational fluid dynamics. Archives of Computational Methods in Engineering 28, 215–261. URL: https://doi.org/10.1007/s11831-020-09437-x, doi:10.1007/s11831-020-09437-x.

Resseguier, V., Mémin, E., Chapron, B., 2017a. Geophysical flows under location uncertainty, Part I Random transport and general models. Geophys. & Astro. Fluid Dyn. 111, 149–176.

Resseguier, V., Mémin, E., Chapron, B., 2017b. Geophysical flows under location uncertainty, Part II Quasi-geostrophy and efficient ensemble spreading. Geophys. & Astro. Fluid Dyn. 111, 177–208. URL: https://hal.inria.fr/hal-01391476, doi:10.1080/03091929.2017.1312101.

Resseguier, V., Mémin, E., Chapron, B., 2017c. Geophysical flows under location uncertainty, Part III SQG and frontal dynamics under strong turbulence conditions. Geophys. & Astro. Fluid Dyn. 111, 209–227. URL: https://hal.inria.fr/hal-01391484, doi:10.1080/03091929.2017.1312102.

Rigal, M., 2022. Low Froude regime and implicit kinetic schemes for the Saint-Venant system. Theses. Sorbonne Université. URL: https://theses.hal.science/tel-03990446.

de Saint-Venant, A., 1871. Théorie du mouvement non permanent des eaux, avec application aux crues des rivières et à l'introduction des marées dans leur lit. Comptes rendus hebdomadaires des séances de l'Académie des sciences, Gauthier-Villars. URL: https://books.google.fr/books?id=mBpjzgEACAAJ.

Smagorinsky, J., 1963. General circulation experiments with the primitive equation: I. the basic experiment. Monthly Weather Review 91, 99–165.

Tissot, G., Cavalieri, A.V.G., Mémin, E., 2021. Stochastic linear modes in a turbulent channel flow. Journal of Fluid Mechanics 912, 1–33.

Tissot, G., Cavalieri, A.V.G., Mémin, E., 2023. Input-output analysis of the stochastic Navier-Stokes equations: application to turbulent channel flow. Physical Review Fluids .

Tucciarone, F.L., Li, L., Mémin, E., Chandramouli, P., 2025. Derivation and numerical assessment of a stochastic large–scale hydrostatic primitive equations model. Journal of Advances in Modeling Earth Systems 17. doi:https://doi.org/10.1029/2024MS004783.

Yang, Y., Mémin, E., 2019. Estimation of physical parameters under location uncertainty using an ensemble^2-expectation-maximization algorithm. QJRMS 145, 418–433.

Zeitlin, V., 2018. Geophysical Fluid Dynamics : Understanding (Almost) Everything with Rotating Shallow Water Models. Oxford University Press.